NASA CONTRACTOR REPORT

NASA CR-41

NASA CR-41

AN X-RAY TELESCOPE

by R. Giacconi, N. F. Harmon, R. F. Lacey, and Z. Szilagyi

Prepared under Contract No. NAS 5-660 *by*
AMERICAN SCIENCE AND ENGINEERING, INC.
Cambridge, Massachusetts
for

NATIONAL AERONAUTICS AND SPACE ADMINISTRATION • WASHINGTON, D. C. • FEBRUARY 1965

AN X-RAY TELESCOPE

By R. Giacconi, N. F. Harmon,
R. F. Lacey, and Z. Szilagyi

Prepared under Contract No. NAS 5-660 by
AMERICAN SCIENCE AND ENGINEERING, INC.
Cambridge, Mass.

for

NATIONAL AERONAUTICS AND SPACE ADMINISTRATION

For sale by the Office of Technical Services, Department of Commerce,
Washington, D.C. 20230 -- Price $3.00

TABLE OF CONTENTS

LIST OF FIGURES

1.0 SUMMARY

17266

An aplanatic total reflection telescope for use in the soft X-ray region has been constructed and tested in this laboratory. The telescope has a collecting area of 2 cm^2, an angular resolution of 1 minute of arc, and a field of view of 40 minutes of arc. The focal length is 64 cm. The grazing angle of incidence on the telescope surface is about 1° for paraxial radiation. This results in an efficiency of reflection of 0.2 percent in the 8 - 12 A region and 5.0 percent at 44 A. These characteristics make it particularly suited to the study of celestial X-ray sources from rocket- and satellite-borne instrumentation.

Author

2.0 INTRODUCTION

Exploration of the solar spectrum in the soft X-ray region below 100A began in 1949 with the work of Burnight (ref. 2) who used ion chambers carried aloft in rockets. Since then observations have been made over the entire spectral range from 100A to 0.01A ($\sim 10^5$ ev), and efforts are currently being made to extend this range further into the gamma ray region.

From these observations there has emerged a general picture of the character of solar X-ray emission which has been summarized by Friedman (ref. 3) in the graph reproduced in Figure 1. The most striking features of the X-ray emission below 30A are its high degree of variability, and its spectral distribution. The variability shows that the sources are localized and associated with flare-producing regions. The spectral distribution shows that these sources have temperatures of the order of a million degrees. These facts show that observations of X-rays can provide information about the structure of the disturbed regions and the mechanism of flares. Thus there exists a need to develop methods of observation by which the structural features can be discerned. This calls not only for improvement in angular resolution, but also for increased effective apertures. It is toward these ends that the work described in this report was directed.

One method of observation, which permits crude structural information to be obtained with large effective apertures, is to measure the current from an uncollimated X-ray sensitive ion chamber or counter exposed to the Sun during a period of time when an X-ray emitting region is carried around the limb into view by the solar rotation. Since the rotation is very slow, this method is only effective with satellites which make possible sustained observations. It obviously suffers from poor resolution, and from the difficulty of distinguishing the geometrical effect of rotation from temporal variations in the emission of disturbed regions.

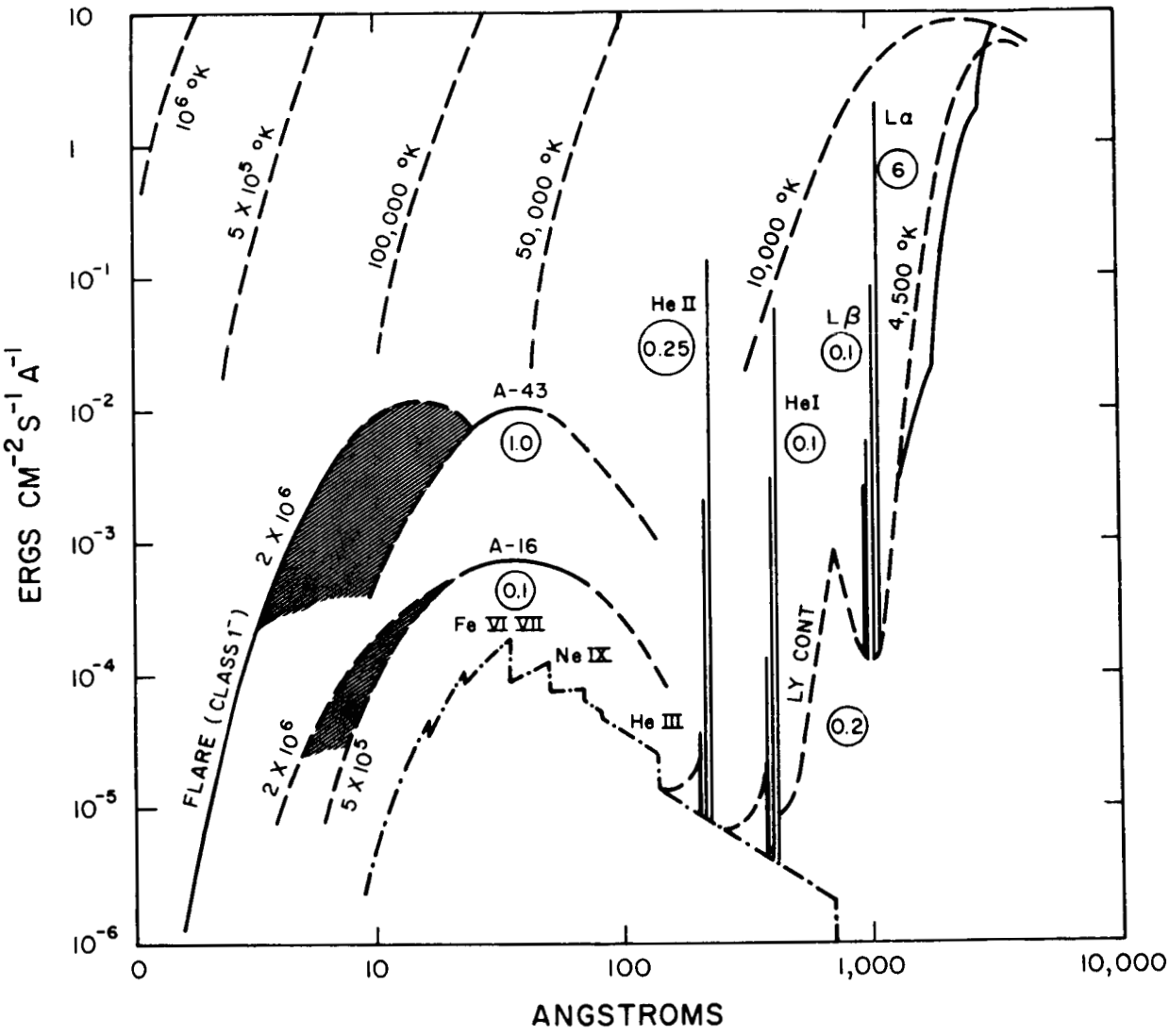

- SOLID LINES REPRESENT ROCKET MEASUREMENTS
- BROKEN CURVES LABELLED WITH TEMPERATURES REPRESENT BLACK-BODY DISTRIBUTIONS
- CHAIN CURVE IS ELWERT'S (1954) THEORETICAL CONTINUUM

From: H. Friedman, Reports on Progress in Physics XVV (1962)
Solar Observations Obtained from Vertical Sounding

Figure 1 Solar Spectral Energy Distribution Below 2000 A

Another method is the pinhole camera with which higher angular resolution can be obtained only through the sacrifice of effective aperture. Friedman, et al. (ref. 3) obtained the first X-ray photograph of the Sun with a pinhole camera mounted on an oriented platform in an Aerobee rocket nose. Since the shutter was left open as the platform rotated about the direction to the Sun, the pinhole image was blurred into a circular pattern. It clearly showed the localized emission of X-rays from an active plage region. Little detail was visible, however, and if the exposure had been made short enough to reduce the rotational blurring to the same order as the inherent angular resolution of the system, then the photograph would have been underexposed.

Two methods exist for the formation of X-ray images which also concentrate the intensity and offer the possibility of reducing exposure times so that rocket rotation will cause less blurring. One of these is the formation of an interference image by a Fresnel zone plate. Such a system, however, is obviously chromatic so that it can be effective only with nearly monochromatic (or filtered) radiation. Furthermore, it does not seem feasible to achieve large collecting areas (very much in excess of 1 cm^2).

Another approach to X-ray image formation is the use of total external reflection at grazing angles of incidence. This had been proposed previously for use in X-ray microscopy, and was recently proposed for use in X-ray telescopy by Giacconi, et al. (ref. 1). Both a collimator and a true image formation device were developed following that publication, and it is the principal purpose of this report to describe these developments, and to set forth the results of tests performed on these devices which demonstrate their great potential value to observational astronomy. As we will show, the image-forming, grazing-angle reflection telescope described below offers the immediate prospect of substantially improved angular resolution in solar X-ray astronomy; and there are excellent prospects for further development.

3.0 TECHNICAL DISCUSSION

In order to improve the present observations in X-ray astronomy, it is evident from the considerations in the preceding section that a need exists for instruments with increased effective aperture as well as improved angular resolution.

In order to accomplish this, it was proposed as early as 1960 (ref. 1) that total external reflection collimators be used from rockets and satellite vehicles provided with pointing controls of the scanning type.

Extensive work was performed during the first phase of this contract to determine the feasibility of constructing collimators of this type and to study their characteristics in the laboratory. The results of this early work are described in ASE-142, dated 6 July 1961. It was realized at that time that improved characteristics could be obtained by use of paraboloidal collimators. Specifically, improved angular resolutions could be expected for a given collecting area.

It was also realized that the development of image forming systems would greatly extend the usefulness of the total external reflection technique. Telescopes could be used for instance from a pointing system without scanning capabilities to obtain simultaneous pictures in X-rays of all objects within the field of view.

For this reason, great emphasis was placed in the program on the development and study of image-forming systems as well as on the techniques of fabrication and polishing of the figured surfaces. These studies and techniques are immediately applicable to the design and construction of collimators.

3.1 Total Reflection

With soft X-rays a telescope or collimator must use reflection, rather than refraction, because of the absorption of this radiation by matter. However, optics using reflection must be designed so that the reflection is at grazing incidence if reasonable reflectivities are to be obtained.

X-rays may be efficiently reflected from surfaces at grazing angles of incidence by total external reflection because the index of refraction of matter for X-rays is less than unity. In general the refractive index may be written as $N = 1 - \delta - i\beta$. If we neglect the imaginary part, we can see from Snell's law that total reflection will occur when the grazing angle of incidence is less than θ_c where $\cos \theta_c = 1 - \delta$, or $\theta_c = (2\delta)^{1/2}$ for the small values of δ involved. Because there is an imaginary part, reflection will not be total, and there will be absorption of the incident power by the reflecting surface. Figure 2 shows how the reflectivity varies with incident angle for various values of β/δ. All calculations of reflectivity are made assuming that the classical laws of optics apply, an assumption which seems to be justified by experiment.

The principal application of this type of X-ray reflection has been in the study of surfaces, X-ray microscopy and attempts to determine the X-ray index of refraction experimentally.

Kirkpatrick and Baez (refs. 4 and 5) showed that an X-ray image could be formed by reflecting an X-ray beam successively at grazing incidence from two spherical surfaces whose tangent planes are perpendicular to one another. Wolter showed that a much larger aperture could be obtained by a mirror system, the reflecting surfaces of which were sections of a coaxial paraboloid and hyperboloid. He made an extensive theoretical study of these systems, but apparently despaired of getting surfaces sufficiently smooth and accurate to attain a resolution approaching that which he calculated theoretically, for no one seems to have constructed such a device for microscopic purposes. We shall discuss this device in detail below with its applications as a telescope.

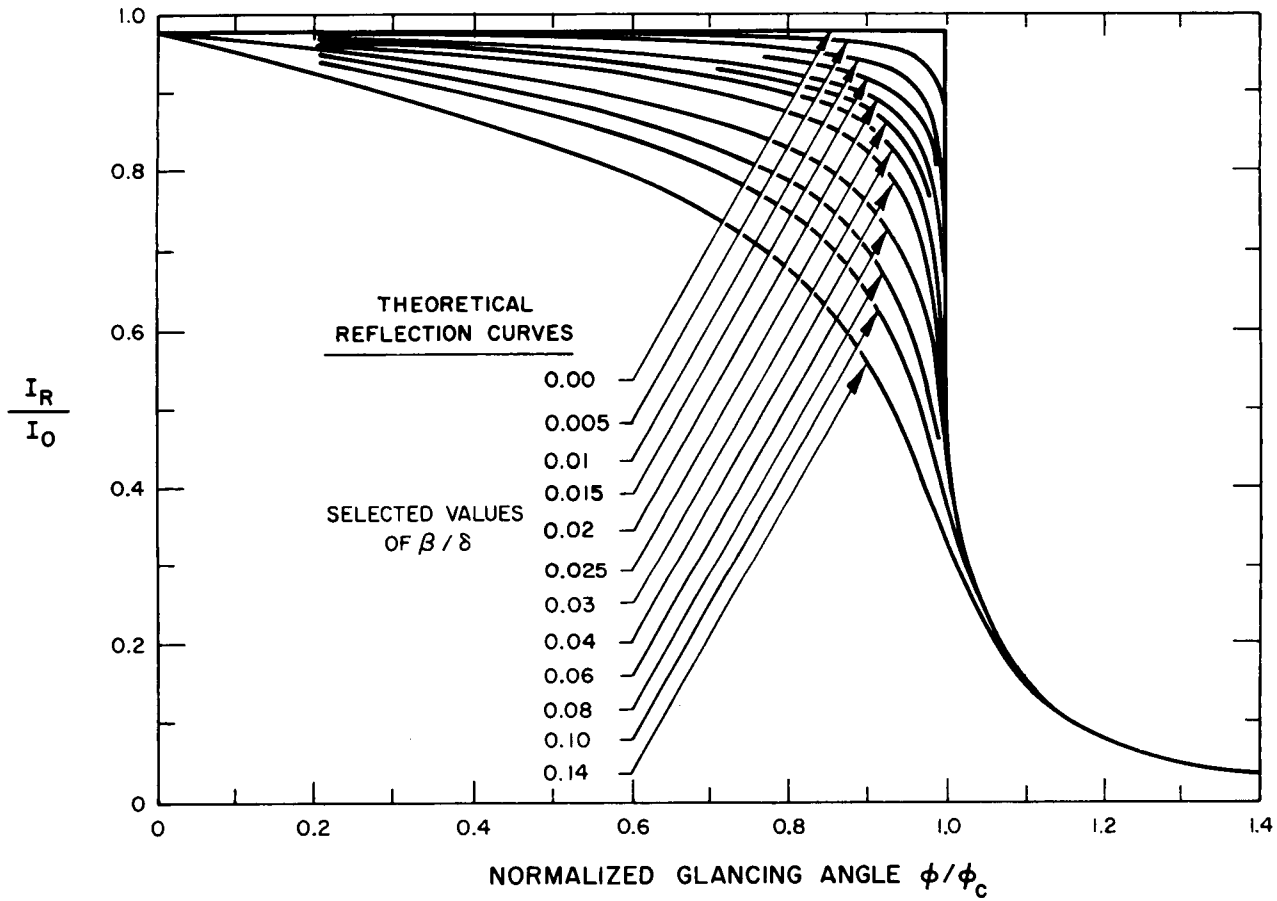

From: R. C. Duncan, L. G. Parratt, AFOSR TN-58-680, ASTIA AD 162 212 (1958)

Figure 2 Theoretical Reflection Curves

3.2 Optics

For an optical system to form images without coma, Abbe's sine condition must be satisfied; that is, the ratio $\sin \alpha / \sin \alpha'$ must be a constant for all rays between an image point and an object point, where α and α' are the angles between a given ray and the line joining the points for the object and image points, respectively. As can be seen from Figure 3a, oblique reflection from one mirror fails completely to approximate this requirement, since α' decreases as α increases. However, with two reflections the condition can be satisfied, as can be seen from Figure 3b. In the system proposed by Wolter (ref. 6), the first mirror is a section of a paraboloid. Paraxial radiation will converge to its focus, but will be reflected again by a mirror whose surface is a section of a hyperboloid coaxial and confocal with the paraboloid. Actually, it is the focus inside the other sheet of the hyperboloid which coincides with the focus of the paraboloid. Because of the geometric properties of hyperboloids, radiation directed toward one focus will, on reflection from the hyperboloidal surface, be reflected toward the other focus, in a manner analogous to the more familiar case of an elliptical mirror. The surface of intersection formed by the incident paraxial rays, extended, and the extension backward of the corresponding rays from the focus where they converge after reflection from the second mirror, is a section of a paraboloid whose focus is the real focus of the optical system. The optical behavior of the two mirror system is the same as that of a single mirror whose surface has the form of this surface of intersection. In general, this surface is an annular region about the center of a spherical mirror.

3.3 Telescope Design

A mirror system similar to the one proposed by Wolter (Figure 4) has been designed and built. The device was machined from aluminum, and the reflecting surfaces were machined aluminum highly polished. It was designed so that the grazing angle of incidence for each surface would be about 1° for paraxial radiation. At that angle of incidence a flat aluminum surface should reflect the aluminum K_{α} line (8.32A) with an efficiency of 60%, as determined experimentally by Hendrick (ref. 7). The diameter of the circle of intersection of the

(a) ONE MIRROR SYSTEM

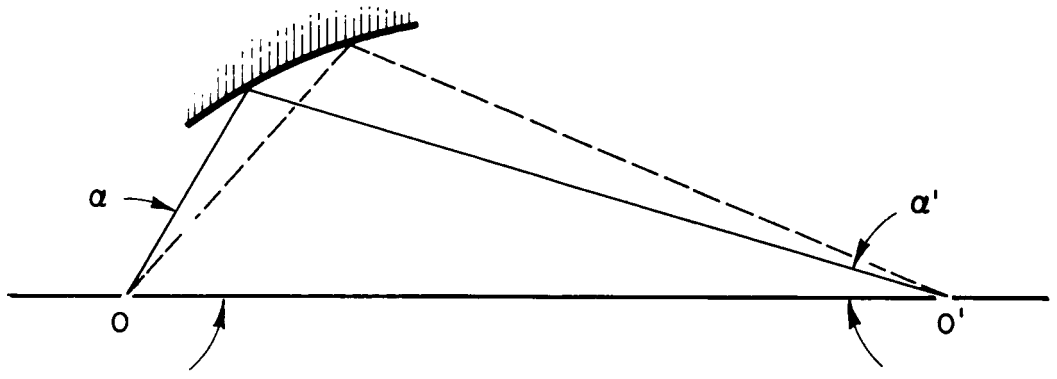

(b) TWO MIRROR SYSTEM

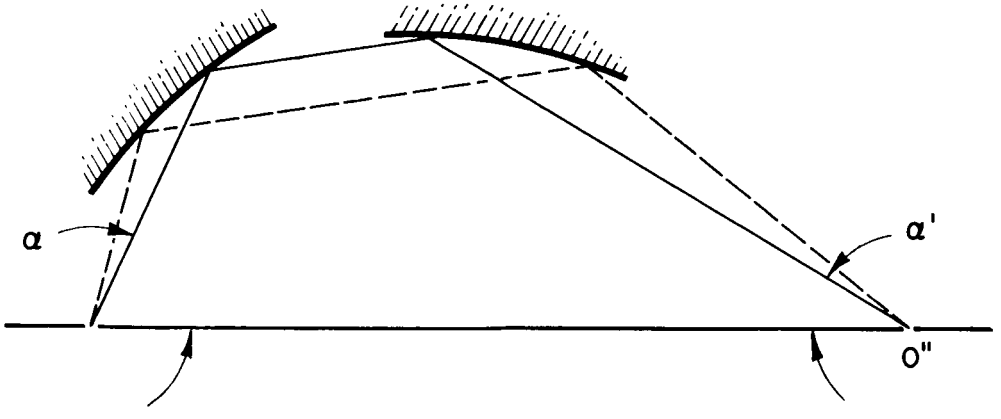

Figure 3 Light Ray Paths for One and Two Mirror Systems

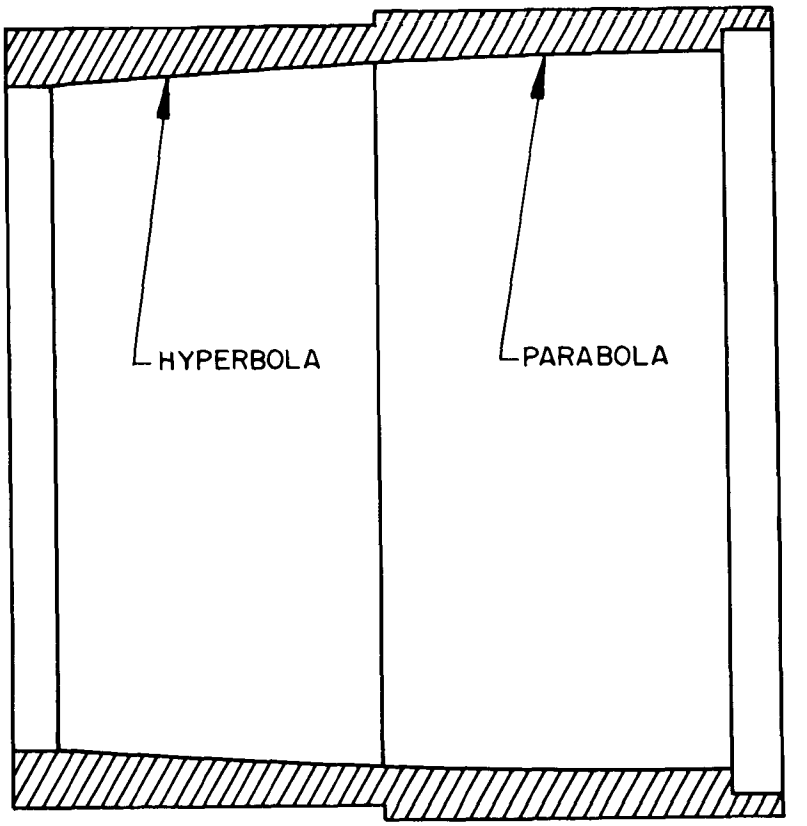

Figure 4 Telescope

hyperboloid and paraboloid was chosen to be 3.5 inches, and the projected area of the section of paraboloid on a plane perpendicular to its axis, the aperture of the system, was chosen to be about 2 cm^2. By the application of elementary analytical geometry suitable equations for the two surfaces are found to be:

$$r = \frac{0.03054636}{1 - \cos\theta} \qquad \text{paraboloid} \qquad (1)$$

$$r = \frac{-0.030583627}{1 - 1.001219832\cos\theta} \qquad \text{hyperboloid} \qquad (2)$$

where r is the distance from the common focus of the two curves to their surfaces, in inches, and θ is the angle between the radius r and the figure axis. θ varies from 1.9964° to 2° for the sections of curves we used. The focal length is 25.027 inches, measured from the center of the circle of intersection mentioned above.

3.4 Ultimate Resolution

The theoretical limit of resolution of this optical system is set by diffraction at the center of the focussed image, and by coma at the edges of the image. From the dimensions of the aperture of the telescope described above, an annulus about .076 cm wide, the diffraction limit of resolution is about 1 second of arc for 44 A radiation, and less for shorter wavelengths. The amount of coma depends on the angle between the incident radiation and the axis of the system. For small angles the angular error due to coma, $\delta\phi$, is given approximately by the equation $\delta\phi = \phi\alpha^2/4$, where ϕ is the angle between the incident radiation and the axis of the telescope, and α is the angle that the paraxial incident radiation makes with the axis at the focus, .07 radians for our case. This formula is adapted from equation (28) of Wolter's paper. For radiation coming in at an angle ϕ of 16 minutes of arc, equal to the angular radius of the Sun, the theoretical resolving limit due to coma is therefore also about 1 second of arc. This will be worsened somewhat because of the finite length of the reflecting surfaces; α differs for rays reflected from various parts of the mirror. Taking all effects together, the theoretical limit of resolution over a field equal to the angular size of the Sun for soft X-rays with the

particular telescope we have described will be a few seconds of arc. Attaining this resolution depends on the practical problems of preparation of the reflecting surfaces.

3.5 Reflection Efficiency

While for reflection of visible light a mirror should be smooth and true to a fraction of a wavelength, this would be impossible to attain for X-rays. Fortunately, it is not necessary. X-rays reflecting at grazing incidence penetrate into the medium a distance of the order of 50 to 100 A, relatively independent of the wavelength of the X-rays (refs. 8, 9, and 10). Because of this, the unavoidable surface inhomogeneities are averaged out in large measure.

Let us consider the requirements on the precision of the mirror surfaces to attain a given degree of resolution, assuming specular reflection. 20 seconds of arc is about 10^{-4} radians, so that if a section mirror is to reflect an incident ray accurately to within 20 seconds, two points 1/10 inch apart of that surface must have their relative attitude accurate to 10^{-5} inch, or to a half wavelength of visible light. This accuracy is beyond what can be obtained with ordinary machining, but is typical of ordinary optical tolerances, where the desired shape is obtained by the averaging process of grinding and polishing, with frequent comparison to standards.

3.6 Collimators

An X-ray reflecting mirror need not be image-forming to be useful. A section of a paraboloid at grazing incidence will serve as a collimator for radiation coming from a given direction, concentrating paraxial radiation down to a point. To be sure, coma is so bad that radiation incident from off axis is imaged into a circle around the focus, but that is no handicap if one wants only to accept radiation from a very small solid angle. The section of paraboloid may be approximated by a conical surface, neglecting the slight curvature of the paraboloid far from its focus. In that case, radiation, instead of being focussed to a point, is concentrated to a small spot whose width equals at best the width of the projected area of the section of cone on a plane perpendicular to its axis (see Figure 5). The angular

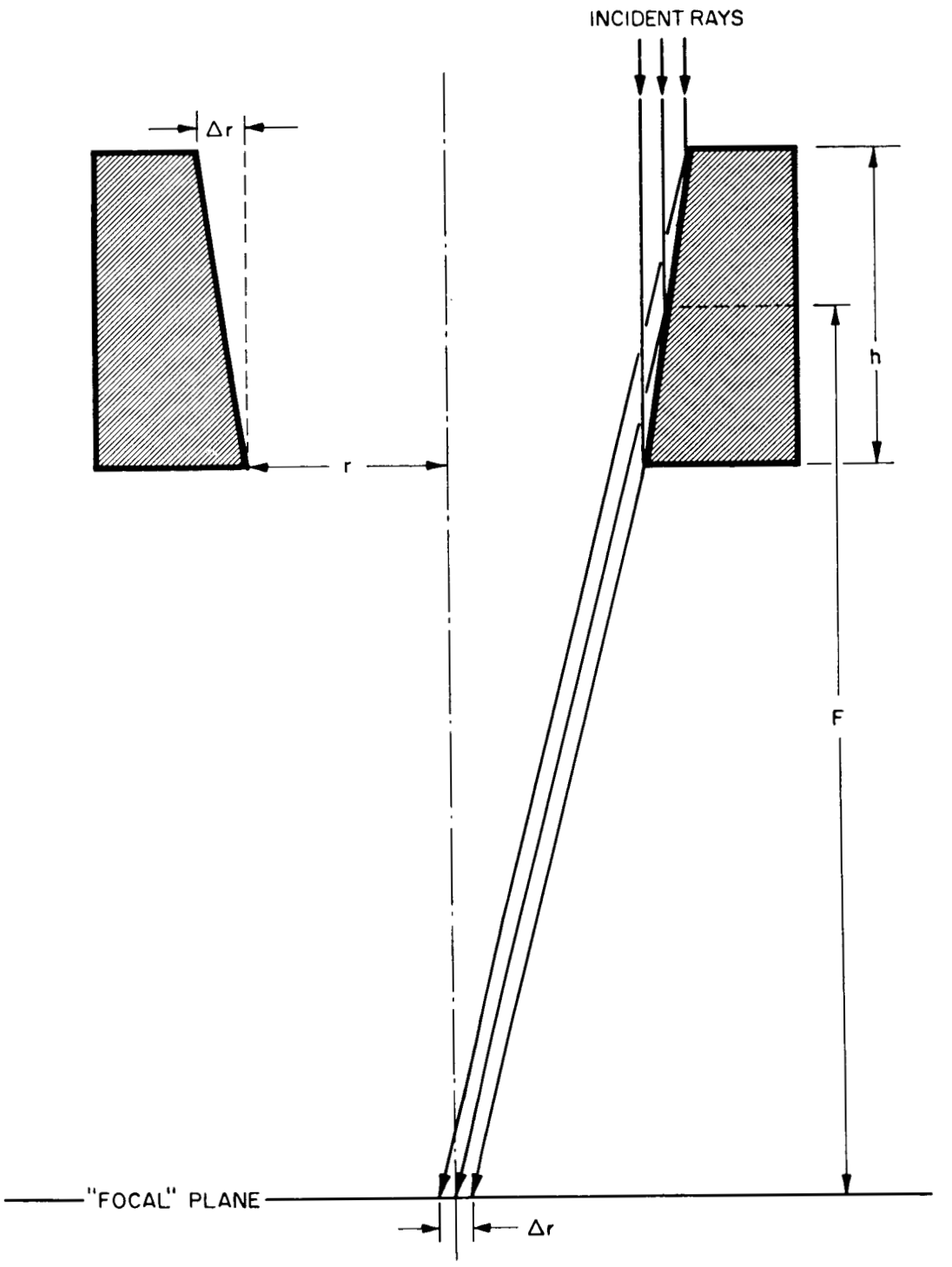

Figure 5 Axial Rays Focused by a Conical Segment

resolution, in radians, is equal to the size of the focussed spot divided by the focal length. [For a paraboloidal (or image-forming device) the size of the spot is in principle limited only by diffraction, while for the cone it is equal to the width of the aperture, as we have said.] For the cone tested, with a "focal length" of 10 inches and an aperture of 1 mm, the resolution is of the order of 4 milliradians, or a little less than 14 minutes of arc.

3.7 Previous Experimental Work

Several investigators have studied specular reflection of X-rays from various surfaces at grazing incidence in recent years. Parratt and others (ref. 8) have studied copper and aluminum films evaporated on glass flats with copper K_β radiation; Hendrick (ref. 7) has studied a variety of freshly evaporated films on optically flat substrates with 8.32 A aluminum K_α radiation. Wuerker (ref. 11) has done the same for 44 A carbon K_α radiation. Henke (ref. 12) has presented a method based on dispersion theory for calculating the index of refraction from the mass absorption coefficient, and a semi-empirical relation for the mass-absorption coefficients of the elements for soft X-rays of all wavelength. This theory predicts the experimental results adequately in the few cases where it has been checked (Figure 6). The method is difficult enough, unfortunately, to require machine computation. However, sufficient engineering data exists for these optically flat surfaces to enable one to design practical optical systems in a reasonable way.

(a) REFLECTION OF Al-K (8.34A) RADIATION OFF ALUMINIZED MIRROR

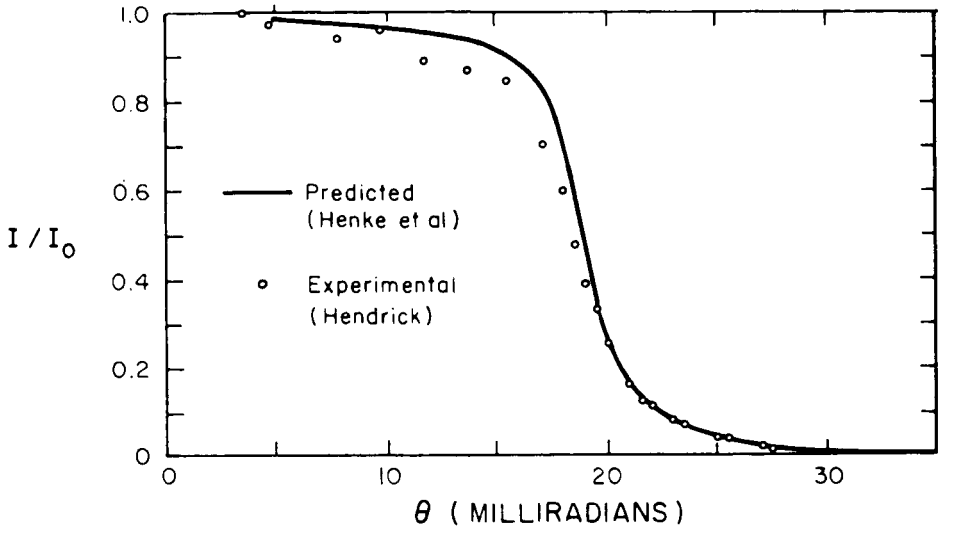

(b) REFLECTION OF C-K (44 A) RADIATION OFF QUARTZ MIRROR

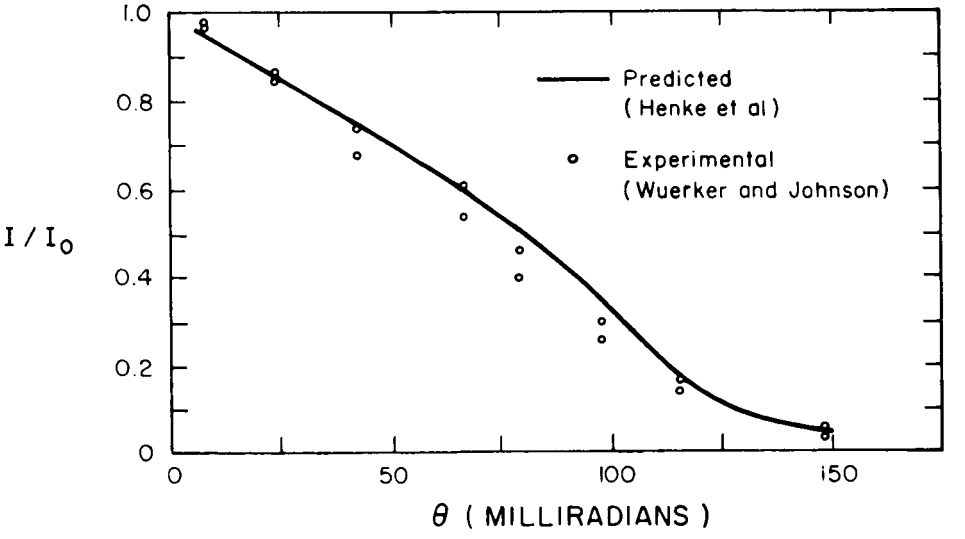

From: B. L. Henke in W. M. Mueller, Advances in X-ray Analysis, Vol. 4, Planum Press, N. Y., 1961

Figure 6 a and b

4.0 EQUIPMENT

4.1 Vacuum System

A vacuum system was designed to minimize the effect of absorption and scattering of soft X-rays. Its size is such that a soft X-X-ray source, a sample to be studied, and detectors may be contained within its volume. It is adequately supported, such that vibration of parts mounted within it will not affect most measurements. The vacuum system has two parts, a pipe and a chamber, joined together. The cycling rate of the system (clean) is approximately two hours. Within this time the pressure in the system is reduced from one atmosphere to 10^{-6} mm of Hg. The leak rate of the system is less than 5×10^{-3} mm of Hg per hour. Both the vacuum chamber and the vacuum pipe (see Figure 7) form part of the permanent facilities program in Space Physics at American Science and Engineering, Inc.

The chamber is approximately 50 inches in inside diameter by 30 inches high. Figure 8 is a photograph of this chamber with its vacuum pumps and electronic control unit. Six manipulators are provided on the chamber. These allow mechanical manipulations inside the chamber without breaking the vacuum. Several high voltage electrical feed-throughs with ceramic insulators are also provided.

The vacuum pipe is built in sections which can be joined to attain a length of 36 feet. The diameter of the pipe is 8 inches and the current length is 30 feet. A valve between the pipe and the chamber and a vacuum pump coupled to the pipe provide independently operating units. This allows the pipe to be let down to air and re-evacuated independently from the chamber. The pipe is furnished with several electrical feed-throughs equipped with high voltage ceramic insulators.

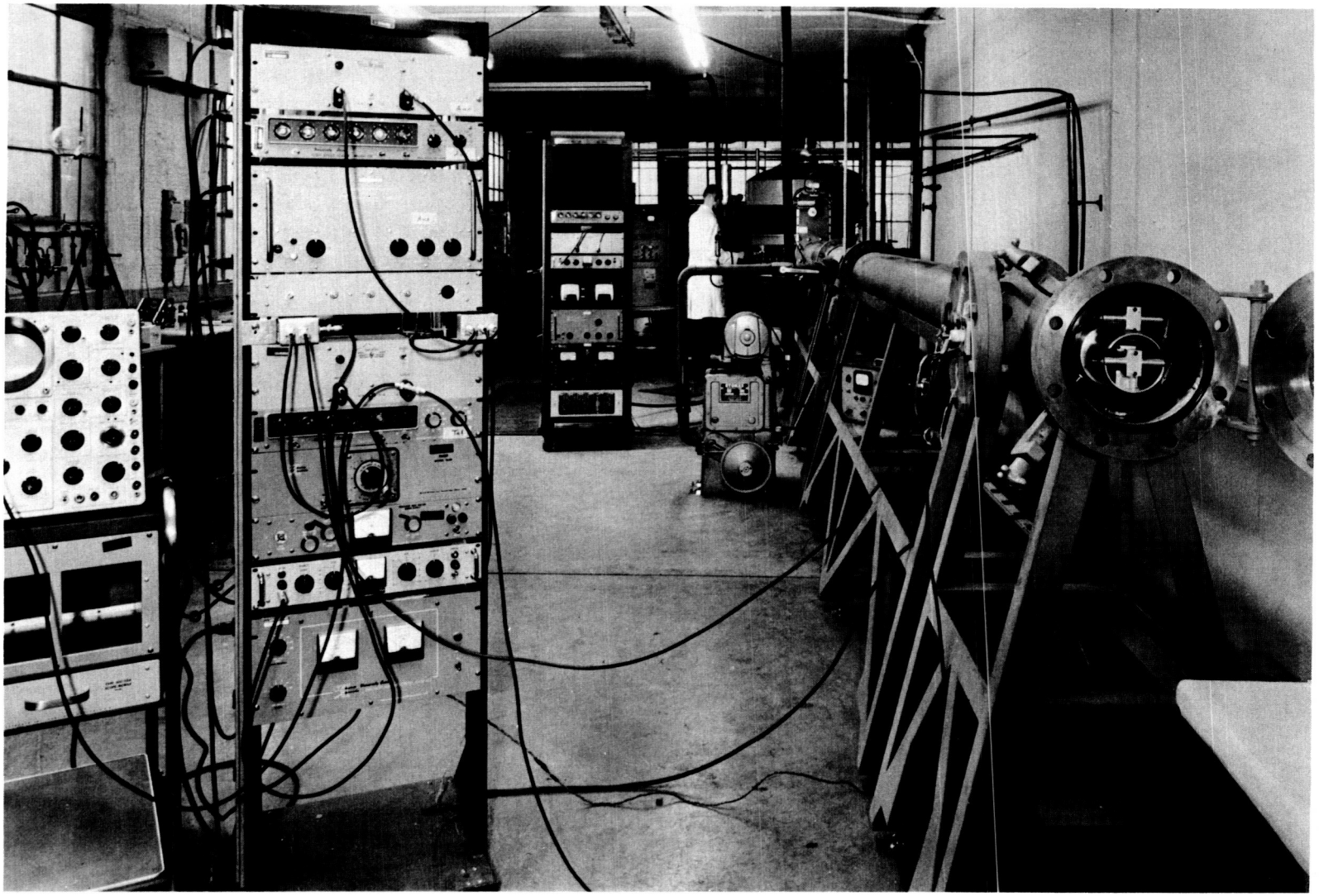

Figure 7 Vacuum System and Electronic Apparatus

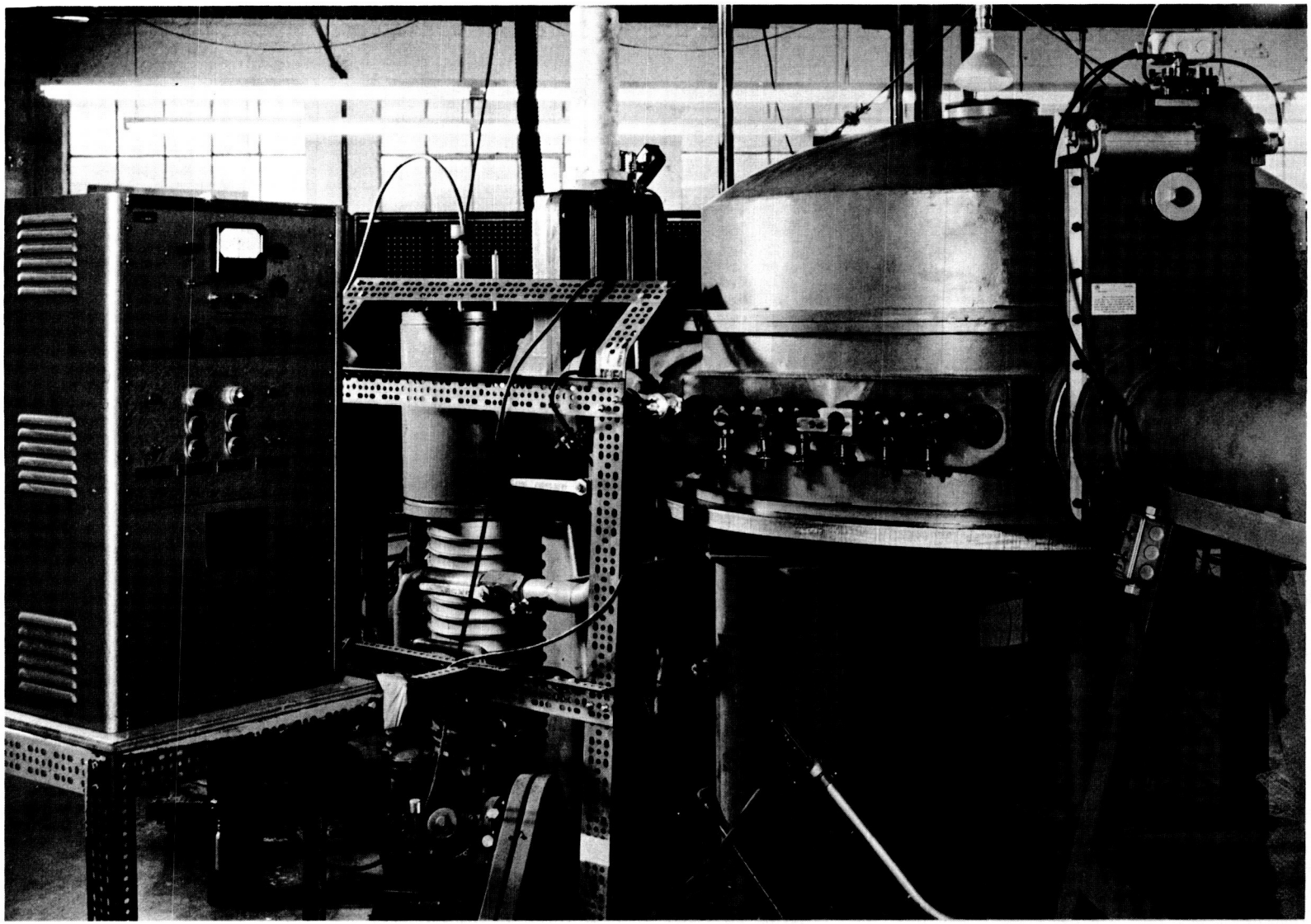

Figure 8 Vacuum System

4.2 Geiger-Muller Counting Filling System

Figure 9 is a photograph of the G-M tube-filling system used in the manufacture and development of thin window G-M tubes having high quantum efficiencies and different spectral responses for different experiments. A leak detector shown on this photograph was employed with this system in the process of producing these tubes.

4.3 Detectors

The detectors chosen for use in this experiment were X-ray photographic film and Geiger-Muller counters.

For photographic techniques Ilford Industrial G X-ray film was inserted in casettes equipped with different filters providing opacity in the visible light region and low absorption for soft X-rays (see Figure 10).

For most experiments performed to date, G-M tubes were employed. This choice was based upon the known quantum efficiency of the tube, their ease of manufacture, reliability, and simplicity of associated electronics.

Figure 11 is a photograph of the two types of G-M tubes developed for use in the experiment. The overall dimensions of these tubes are approximately 6 inches long and one inch in diameter. The body of the tube is made of stainless steel. The $7.91 \pm .02$ mm^2 circular window area at the center of these tubes was covered with 0.25 mil thick mylar (corresponding to 0.78 mg cm^{-2}). The counters were filled with 493 mm pressure of Argon and 7 mm pressure of ethyl formate quench. The plateau region of these tubes was between 1250 - 1500 volts. Their quantum efficiencies were approximately 46% at 8.3 A and 7% at 44 A (Figure 12).

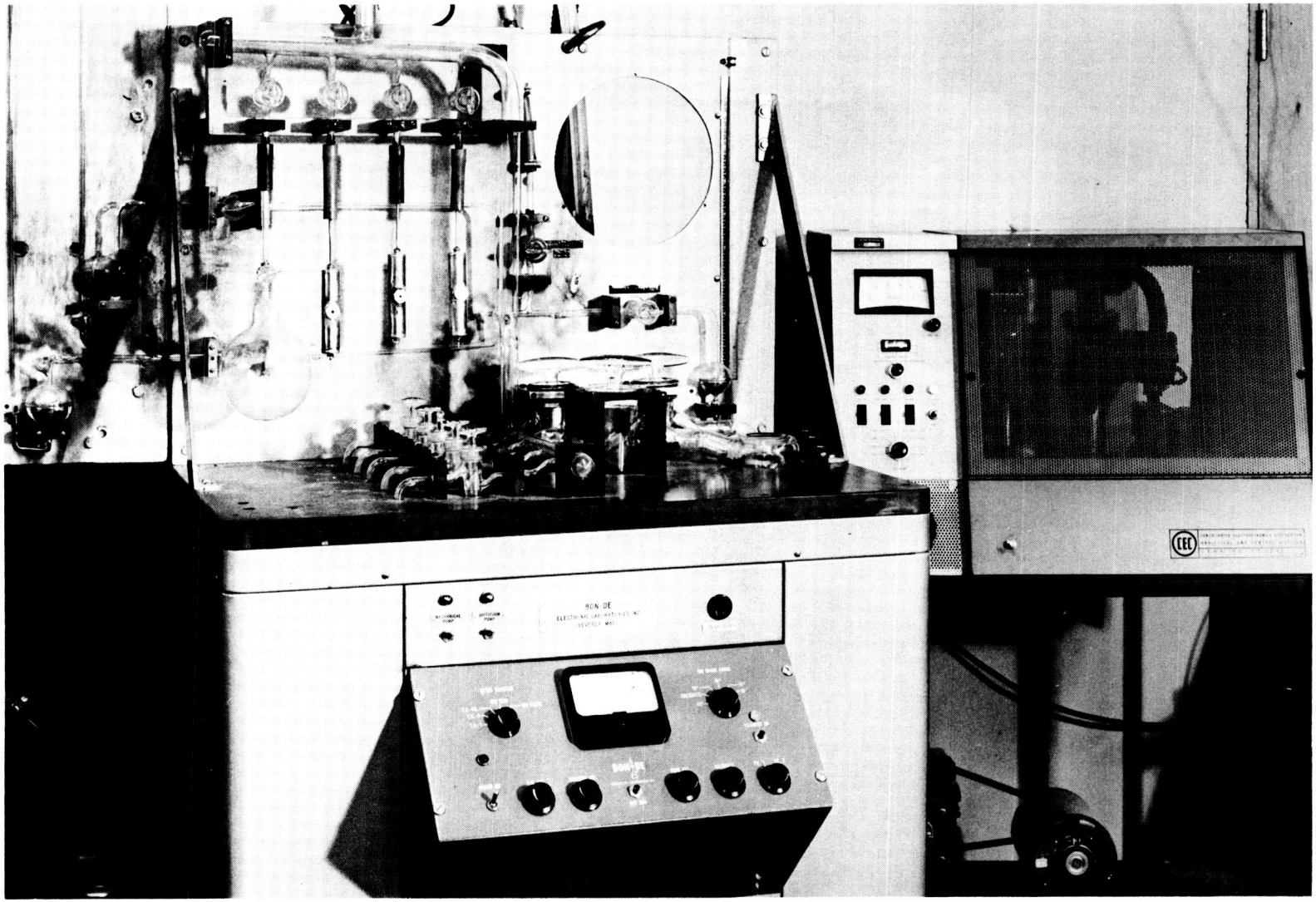

Figure 9 Geiger Tube Filling System and Leak Detector

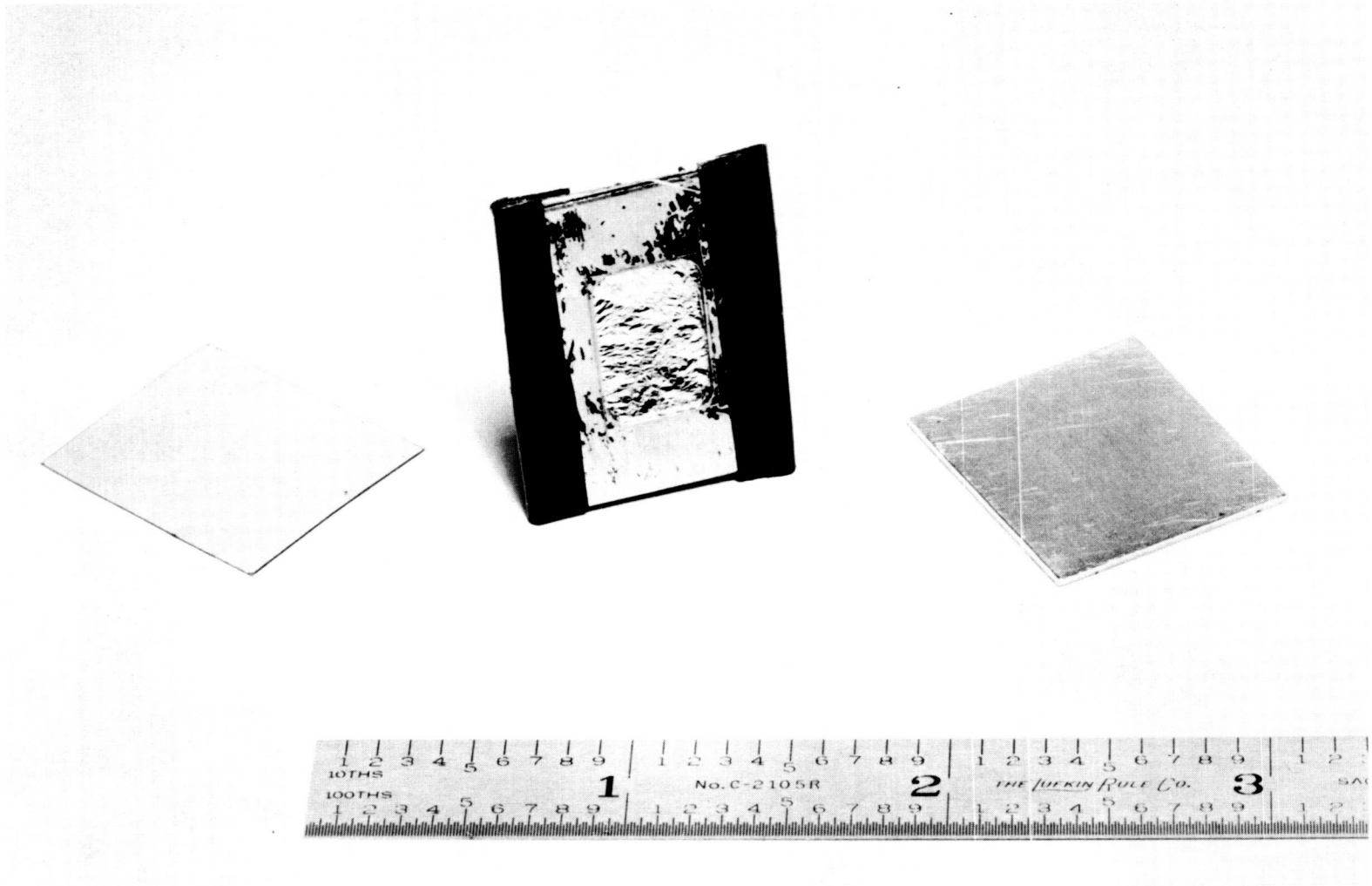

Figure 10 X-Ray Film and Cassette

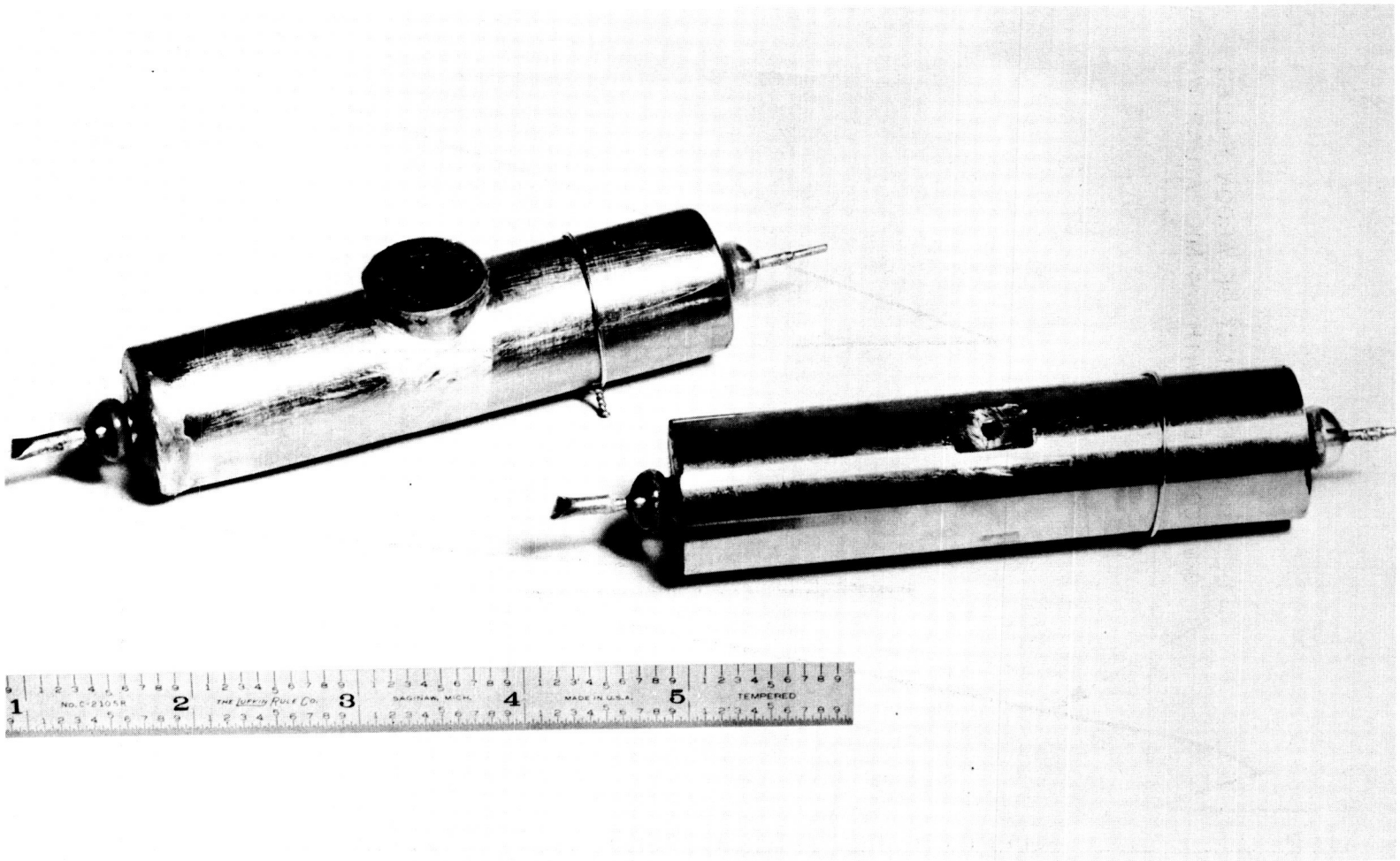

Figure 11 Geiger Counters

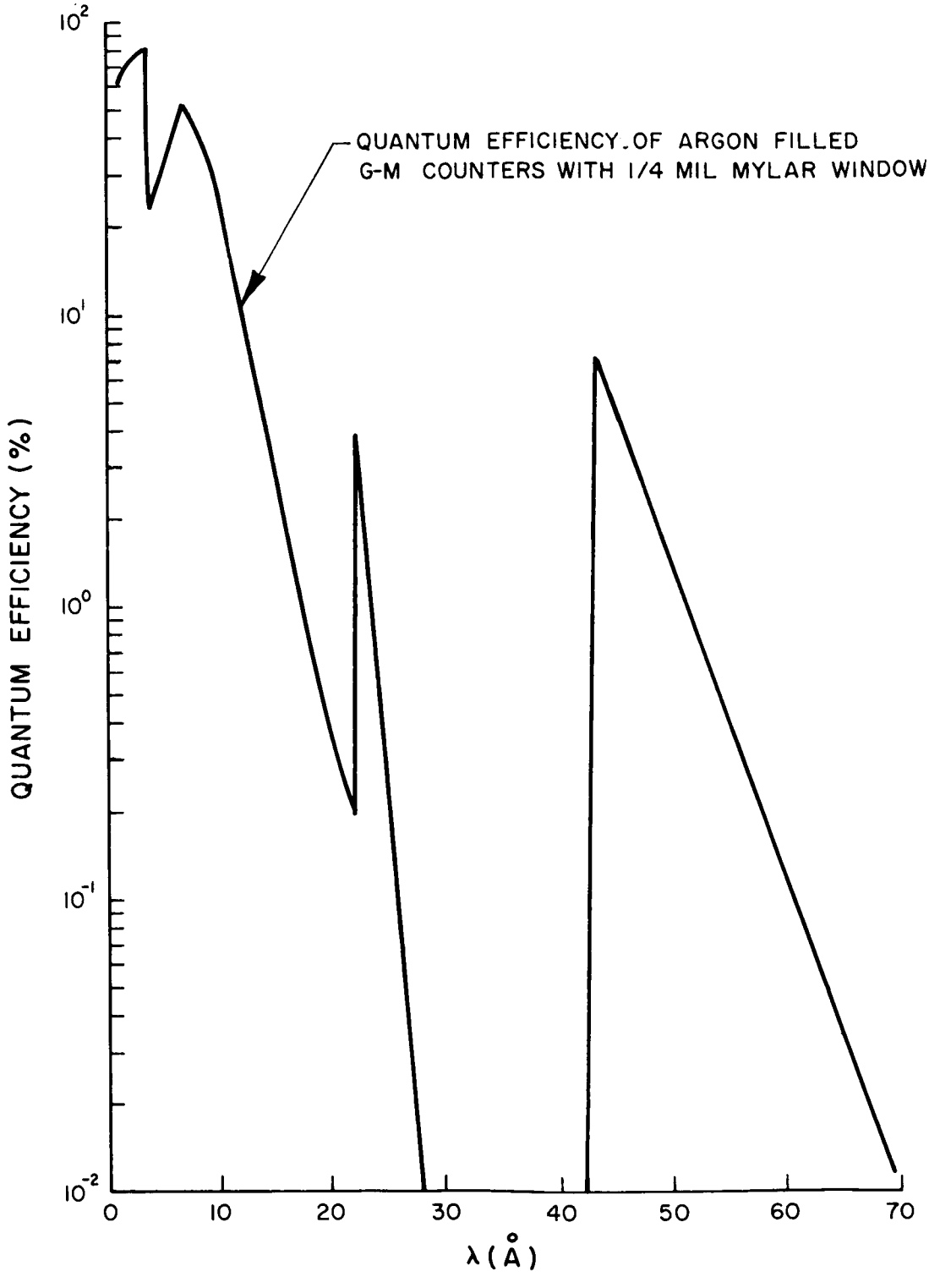

Figure 12 Efficiency of G-M Counters vs Wavelength

4.4 X-Ray Sources

Two types of X-ray sources were designed and constructed in order to meet the experimental requirements (production of high intensity long wave-length X-radiation, demountable source, movable platform, freedom from sputtering and contamination of target materials).

Figures 13 and 14 are photographs of the X-ray source assembled and demounted. The simplicity of the design is evident from these figures. The basis of this open structure X-ray source is a simple electron gun with a thoriated tungsten filament whose beam is focused upon a carbon or aluminum target, thus producing a point X-ray source. A one element, short focal length electron lens was designed. Figure 15 shows the essential components of this lens. The anode and cathode are concentric spherical surfaces. The electron source is a tungstem filament mounted at the cathode. The focal point of this lens is on the surface of the target. Holes are provided in the anode through which the produced X-ray may pass. The assembled structure is mounted on a movable platform which can be adjusted by a screw operated from outside the vacuum chamber to traverse the field of view of the telescope.

This arrangement was placed in the chamber evacuated to a 10^{-6} mm pressure. The anode to cathode potential was 1500 volts for the carbon target and 3000 volts for the aluminum target. The beam current was 0.1 ma and 1 ma, controlled by varying the temperature of the emitting filament. An X-ray intensity of the order of approximately 1000 photons per 10^{-3} radians per second was obtained.

Figure 16 is a photograph of another X-ray source. This source was designed and constructed to produce a high intensity extended X-ray emitter. The size of the source was approximately 1 1/4 inches by 1/4 inch forming a semi-elliptical area.

4.5 Electronics

Figure 17 is a photograph of the electronic components used in the experiment. Most of the apparatus is commercially available.

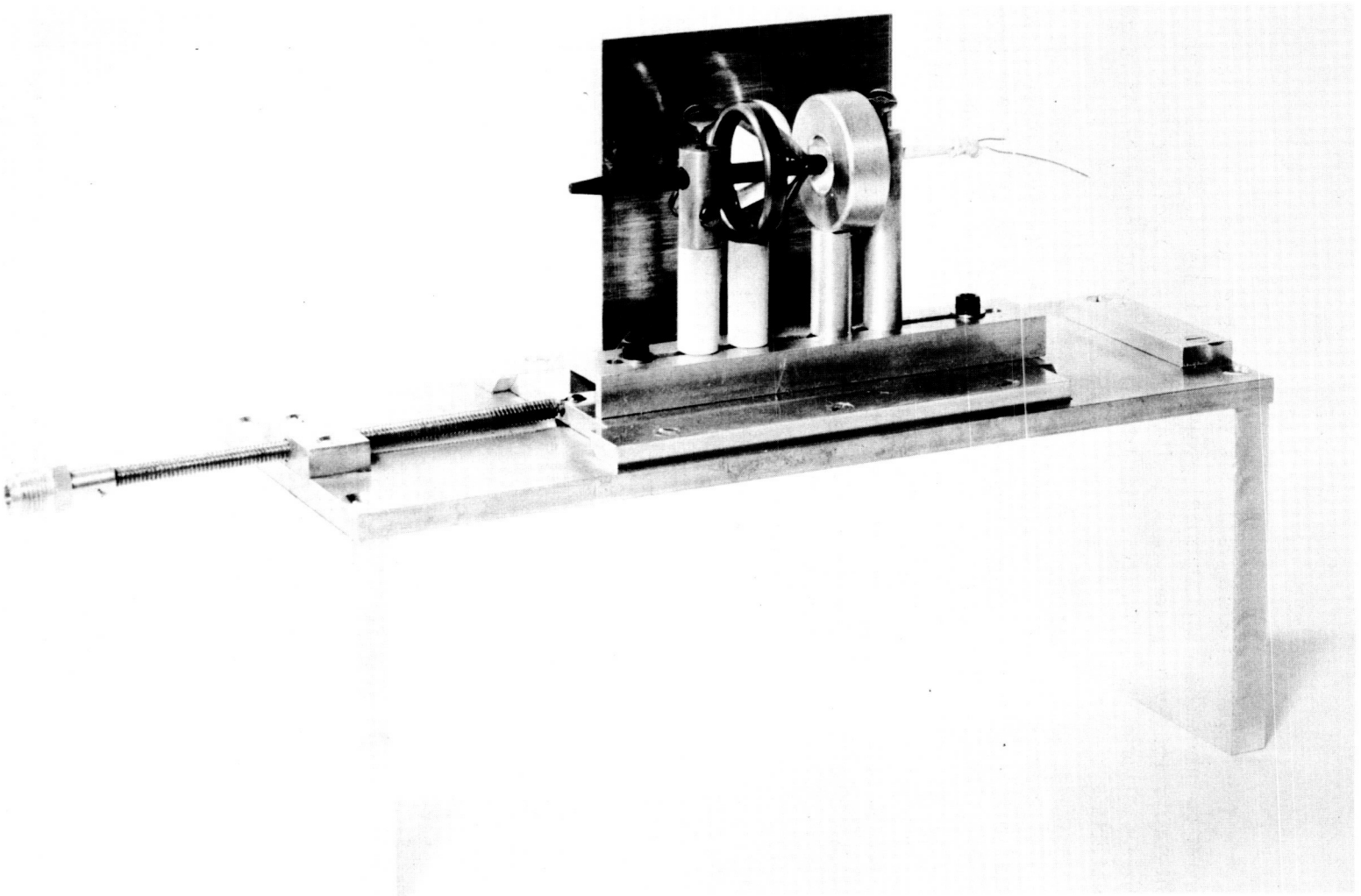

Figure 13 Point X-Ray Source on Movable Carriage

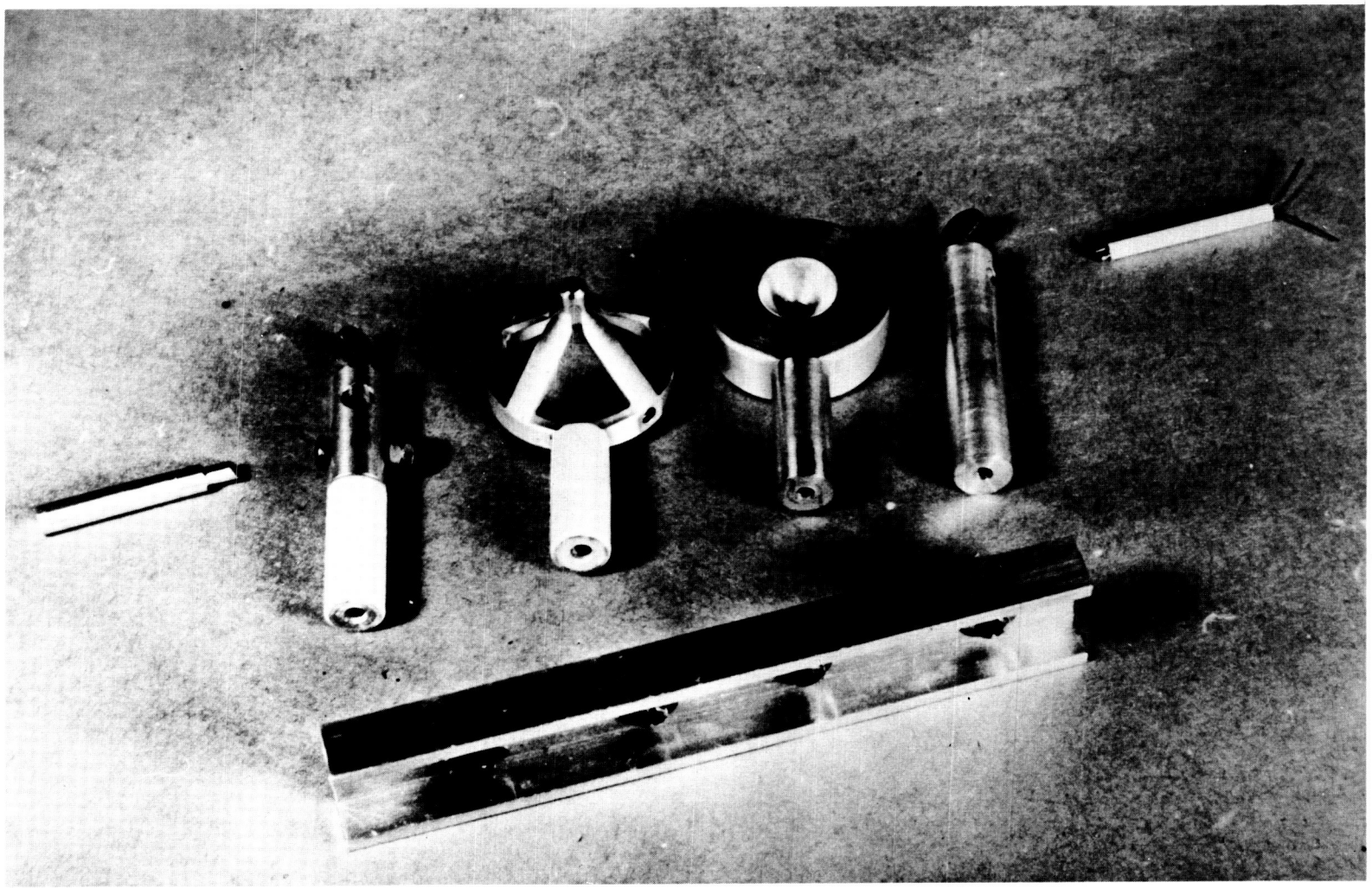

Figure 14 Exploded View of Point X-Ray Source

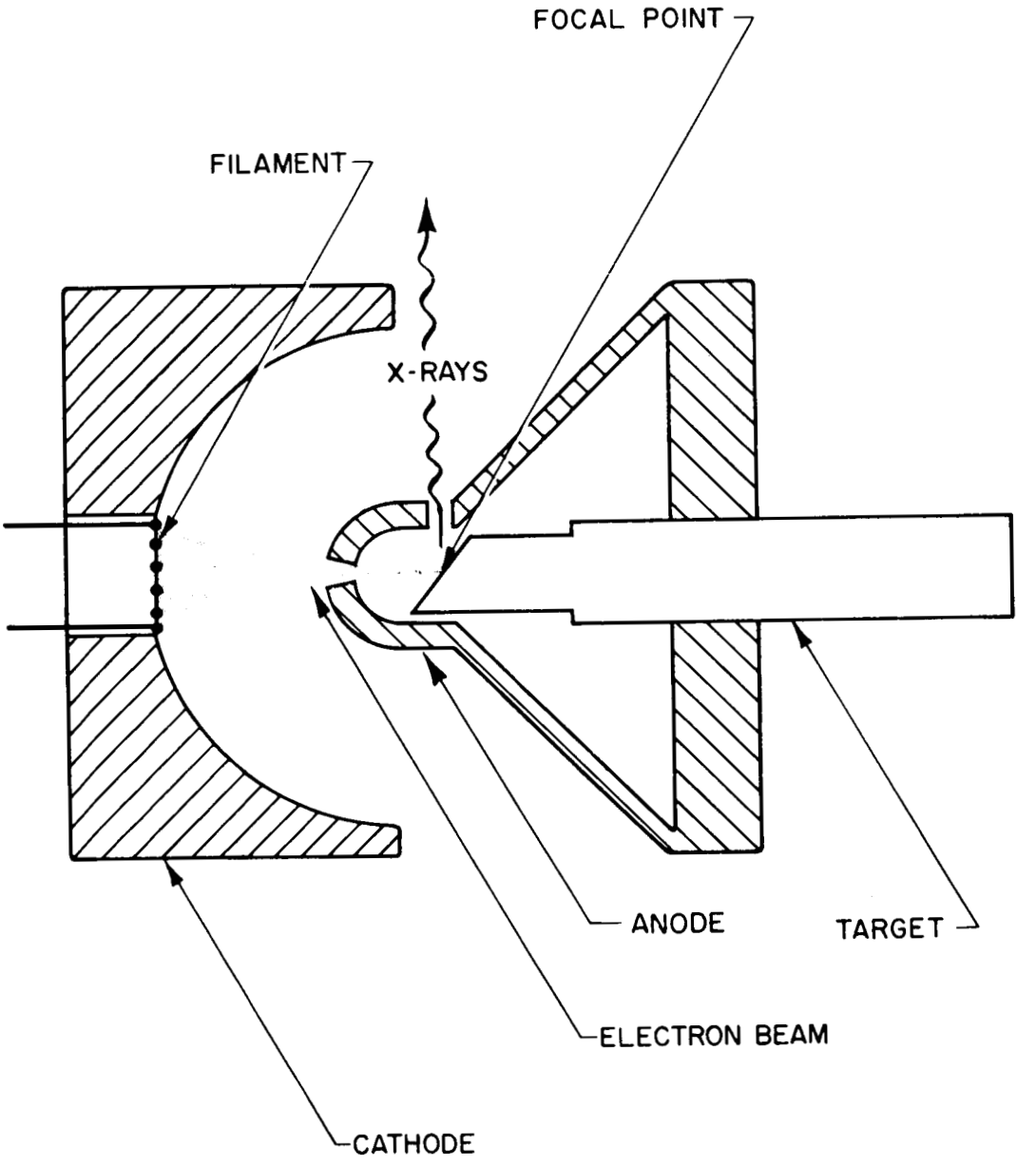

Figure 15 High Intensity Soft X-Ray Source

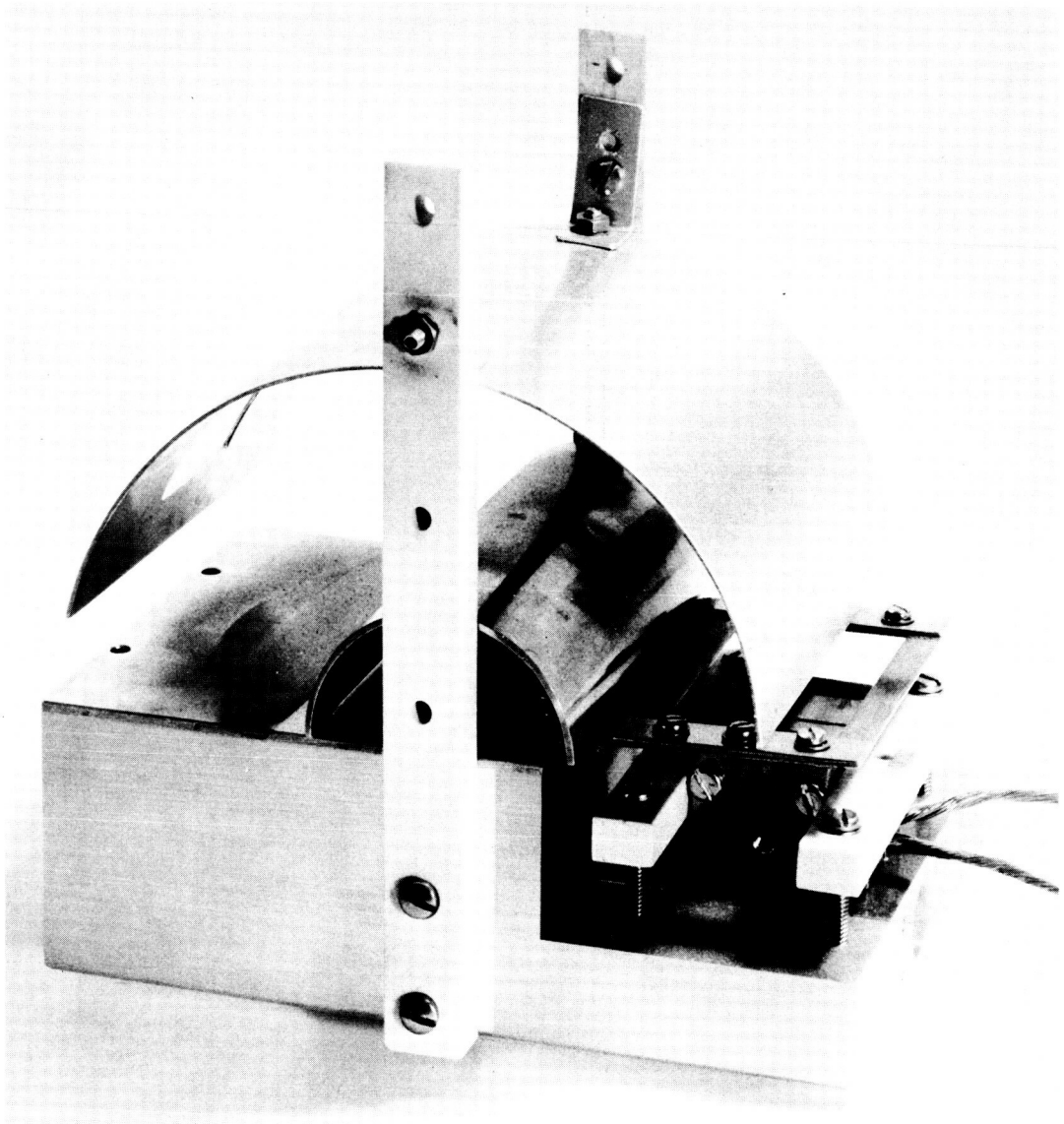

Figure 16 Large Area X-Ray Source

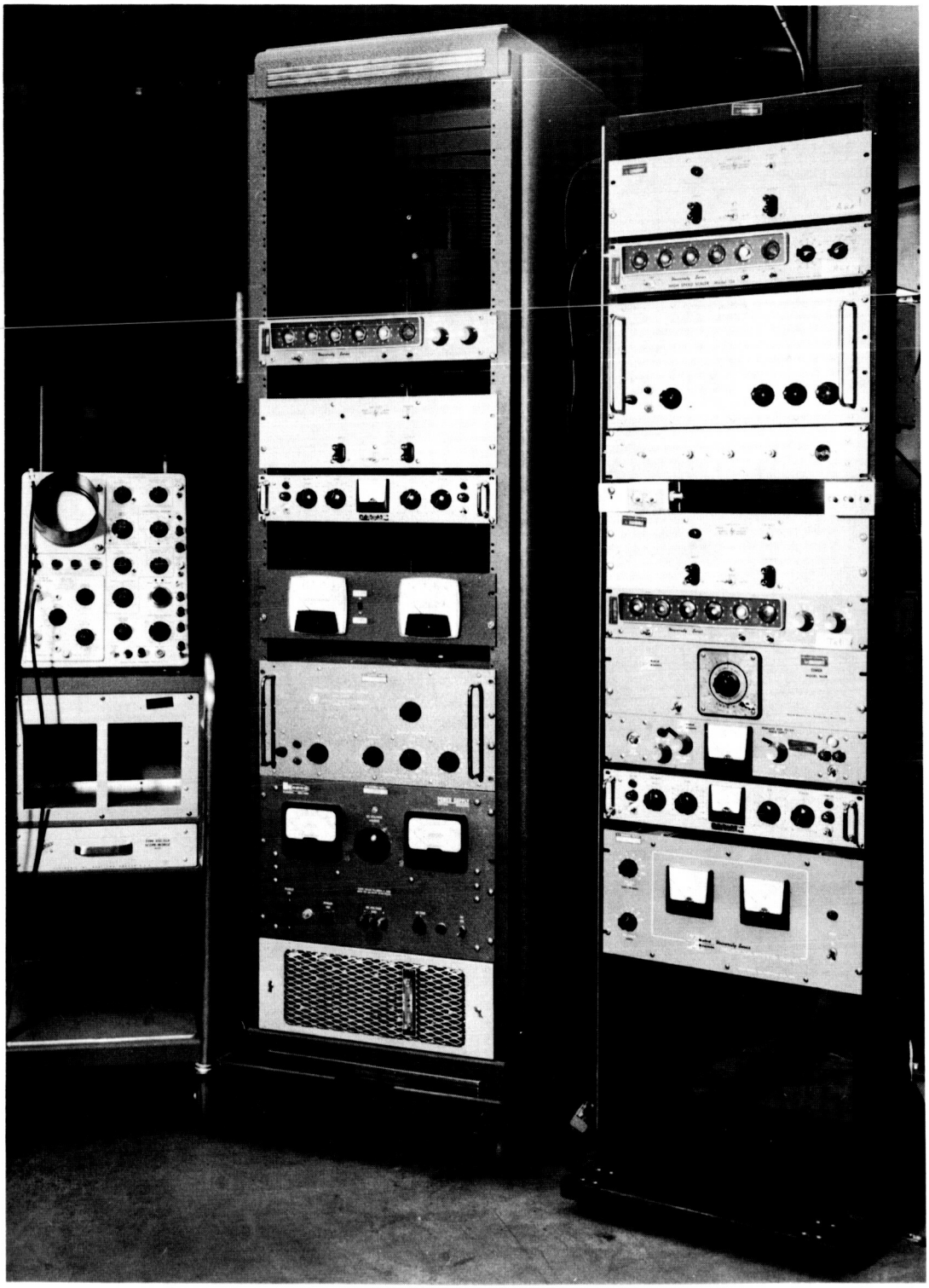

Figure 17 Electronic Apparatus

The equipment consists of the following components:

1	Kepco KM 235-15A voltage regulated power supply
1	Northeast RE 10010 regulated high voltage supply
1	Northeast RE 2003 regulated high voltage power supply
2	Fluke 412A high voltage d.c. supply
3	Hewlett-Packard 420 AR amplifier
3	Baird-Atomic 134 high speed scaler
1	Tektronix 545 A Oscilloscope

4.6 Optical Equipment

4.6.1 Goniometer. For the design and development of X-ray collimators and telescopes, it is necessary to determine the shape of the reflectance curve for various wavelengths, angle of incidence and materials. A General Electric SPG spectro-goniometer (Figure 18) was used as a convenient device for precise angular measurements. This goniometer may be used to measure angles to within 3×10^{-4} radians. This degree of precision is well within the 5×10^{-4} radian resolution required for a useful X-ray collimator or telescope. The goniometer, as purchased, could not be used directly for the proposed experiments. Major modifications were necessary in order to adapt it to a reflectivity measuring instrument. Modifications included providing supporting structures for an X-ray source, the sample to be studied, and the detector. It was also necessary to prepare this device for use in a vacuum. Most of the adjustments could be aligned by using external feed-through manipulators on the vacuum system. The goniometer was used extensively during the first phase of the research program in studying properties of surfaces.

4.6.2 Collimators. Identical steel and glass cone collimators (Figure 19) were designed and constructed. The thickness of each collimator is 1.227 ± 0.001 inches, and its outer diameter is 3.150 ± 0.001 inches. The interior surface of each collimator is conical; the annular diameters are 1.456 ± 0.005 inches and 1.378 ± 0.005 inches. The angle of the cone is 2°. The projected area of the cone, viewed along its axis, is approximately 1 cm^2. The conical segment to the right in Figure 19 is made of glass; its interior surface has been optically polished. The conical segment to the left of Figure 19 is a steel replica of the glass cone.

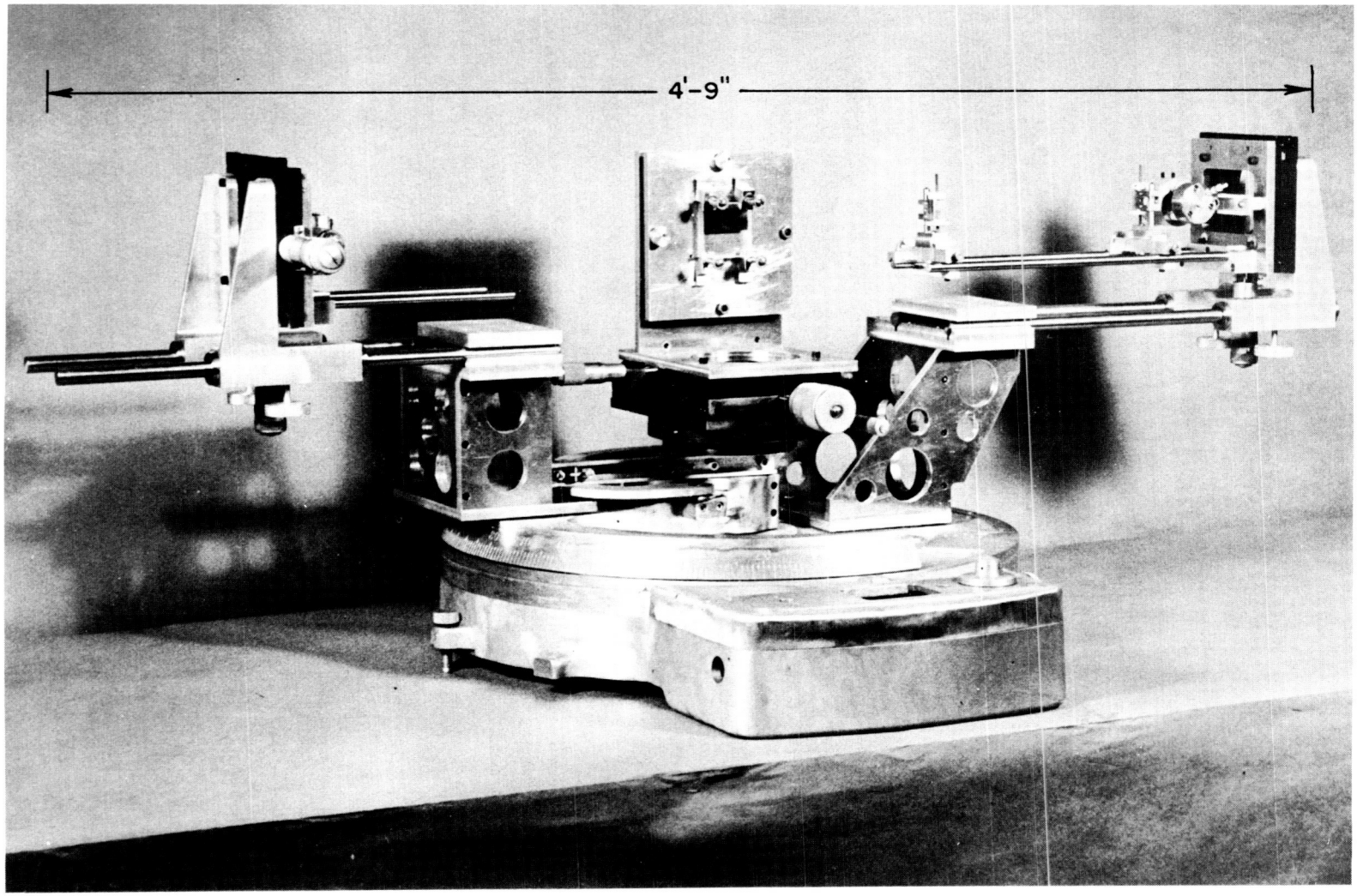

Figure 18 Goniometer for X-Ray Reflection Studies

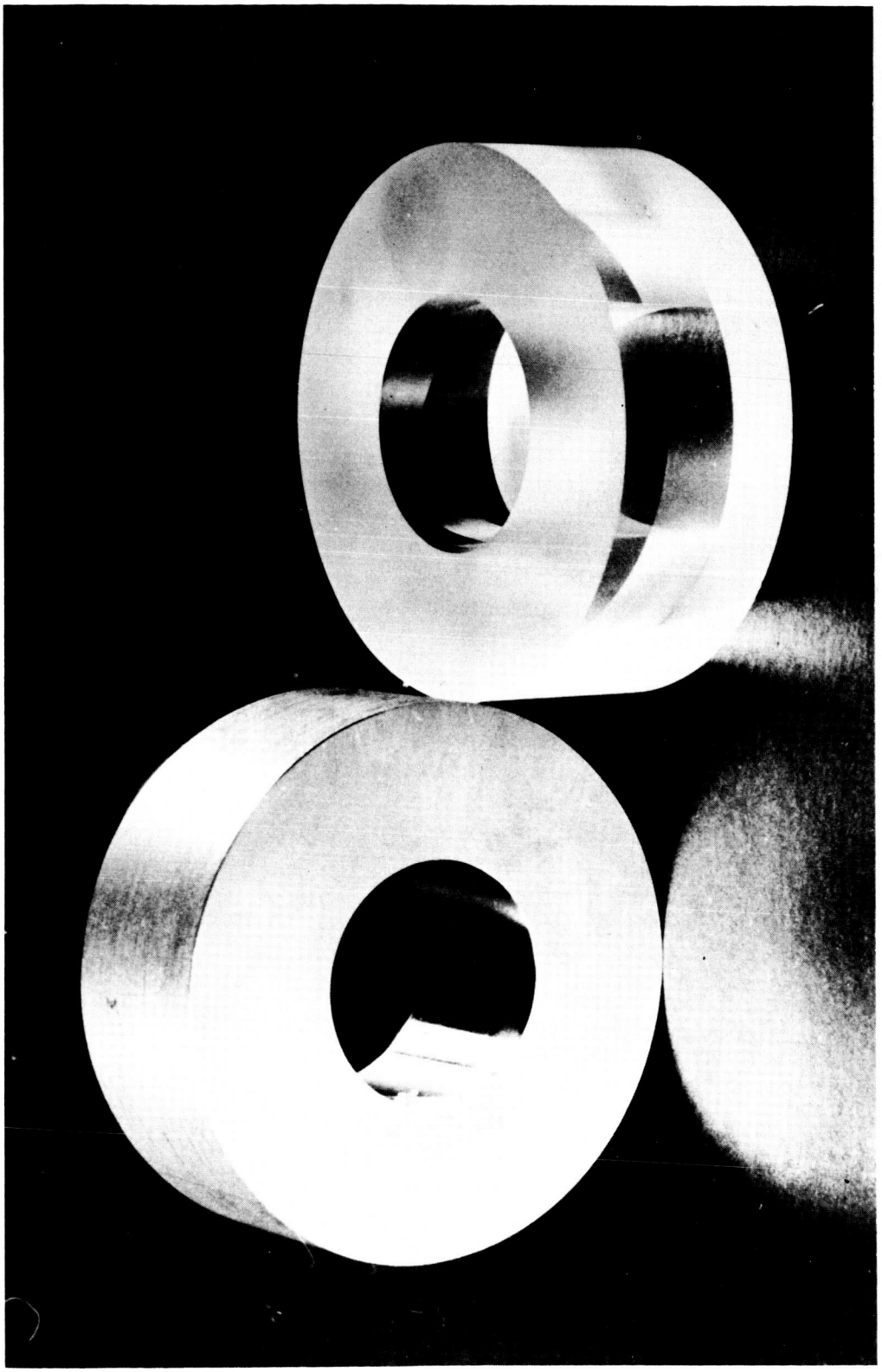

Figure 19 Steel and Glass Cone Collimators

Figure 20 shows the assembly used in the investigation of the X-ray reflecting properties of the above conical segments. The parts are the following from left to right: stop, glass cone, cone holder, mounting, sliding tube for focusing with auxiliary G-M counter set on top, and G-M counter in its holder. The stop has a ring-like opening to intercept direct X-radiation and to allow radiation to impinge on the telescope at grazing angle of incidence.

The cone holder provides accurate alignment to the axes of the cone and the apparatus when it is inserted into the mounting. The mounting is an aluminum conduit with four adjustable legs; it is the frame of the apparatus and about 9 inches long. A diaphragm with a one millimeter hole on it is set inside of the focusing tube. This is placed inside the mounting. The collimator assembly is inserted at one end of the long vacuum pipe and aligned on an X-ray source 33 feet away at the other end of the vacuum chamber. The beam of X-rays was concentrated by the reflection to a spot one millimeter in diameter on the axis about 10 inches behind the cone. The alignment was checked by replacing the X-ray source with a point light source and adjusting the supports and the focusing tube until all the light reflected by the cone passed through the hole in the diaphragm (Figure 21).

A G-M counter was placed at this point supported by the niche cut out on the focusing tube so that the window of the G-M counter was in contact with the diaphragm. An auxiliary G-M counter was placed on top of the apparatus in such a fashion that its window had a direct view of the X-ray source; this monitored the X-ray flux impinging on the telescope or collimator.

4.6.3 Telescopes. Several telescopes were constructed; some of them are shown in Figure 22. For these devices the efficient reflection of soft X-rays, as for the cone collimators, depends on the small angle of incident radiation. For the construction of the telescope, aluminum was chosen for its durability, cost, relative ease of manufacture of complex surfaces by precision machining and ease of polishing.

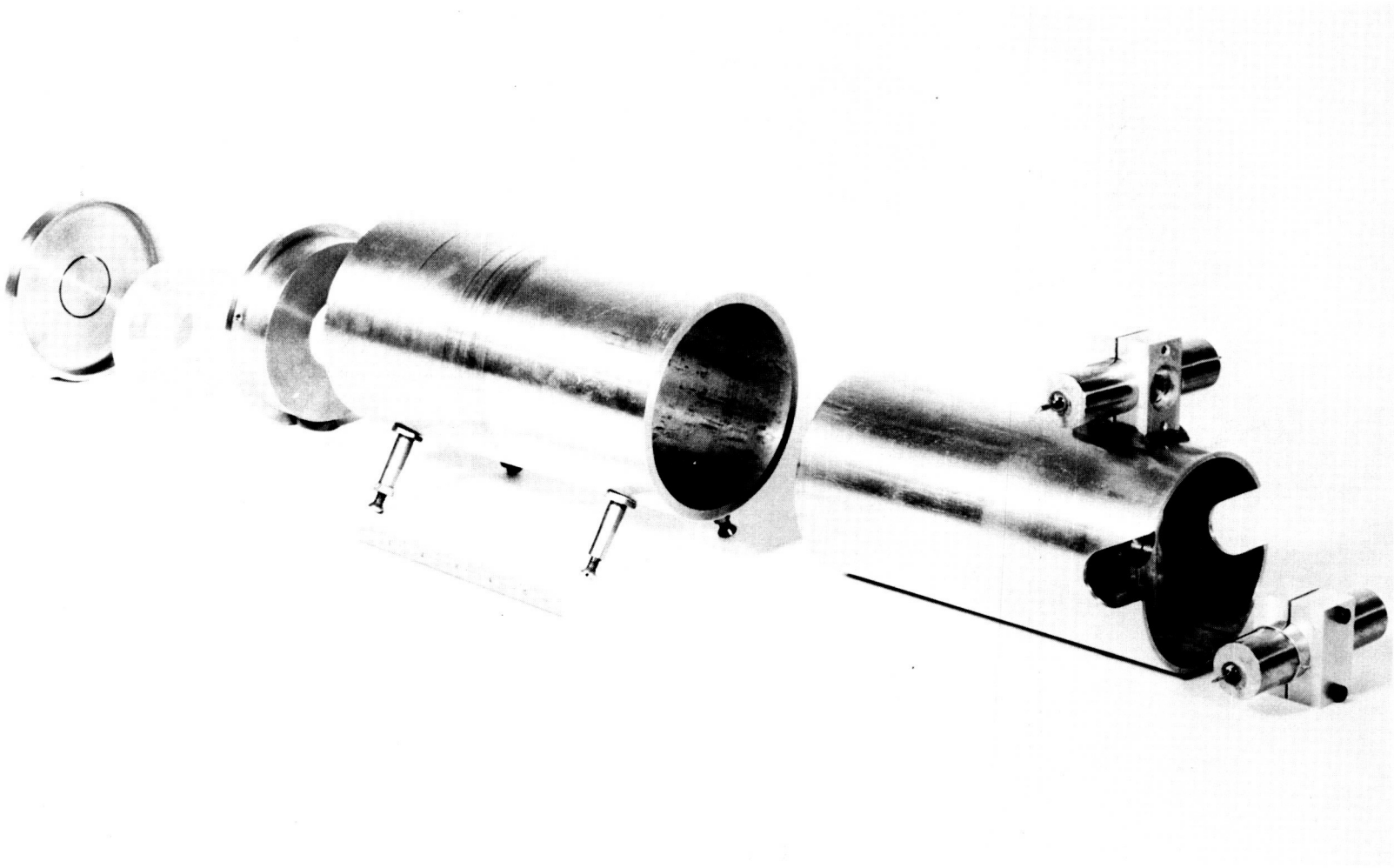

Figure 20 Glass Cone Collimator Assembly

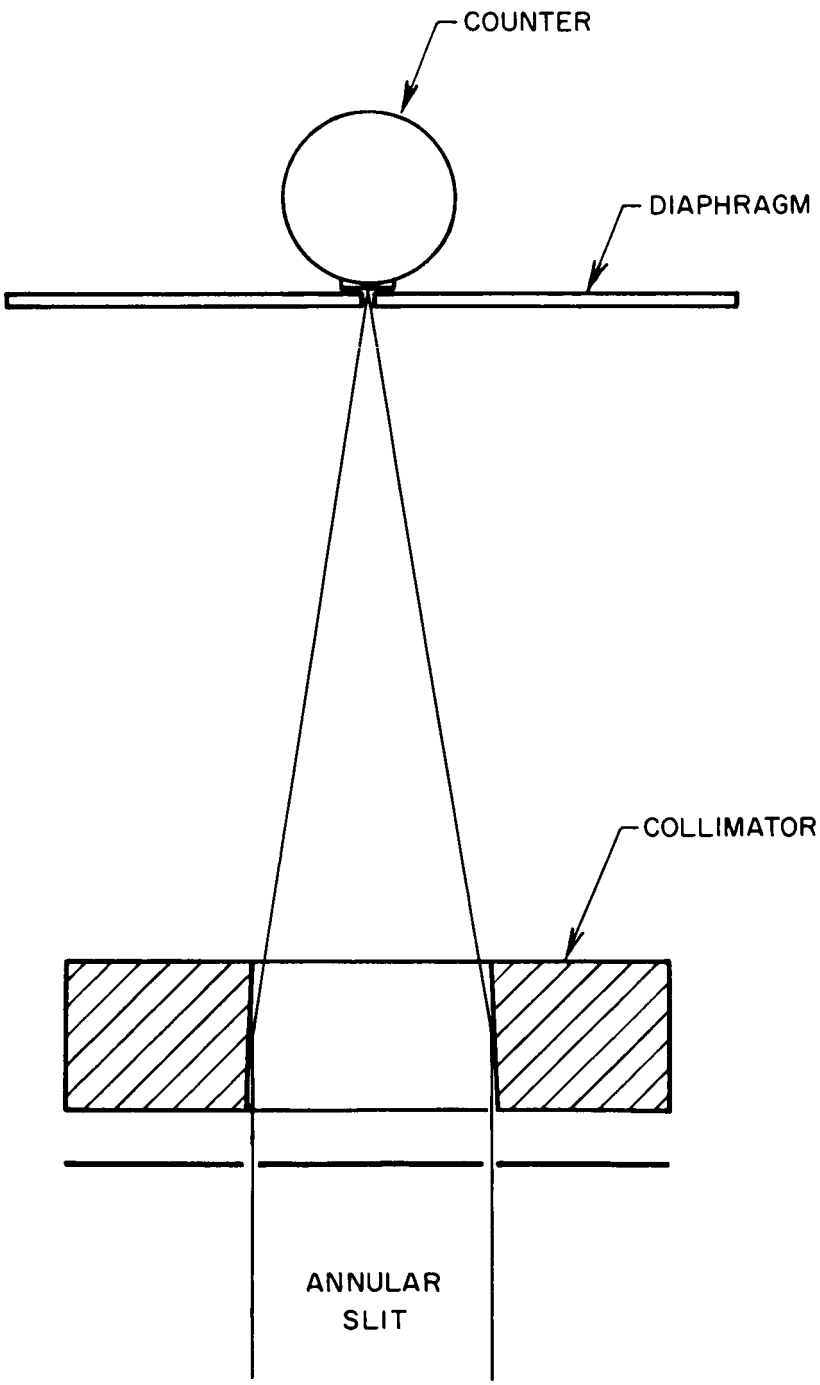

Figure 21 Glass Cone Collimator

Figure 22 Aluminum and Cast Epoxy Telescopes

The first part of the curved surface of the telescope (Figure 4) is a section of a paraboloid chosen so that radiation parallel to the axis of the device is incident at an angle of about 1^{o}. Radiation reflected from this surface is then incident on a section of a hyperboloid so chosen that the grazing angle is also about 1^{o}, and so that the paraboloid and hyperboloid are confocal. After the second reflection, the radiation is focused to the other focal point of the hyperboloid, which is closer to the reflecting surfaces. Thus, a shorter overall focal length is achieved than could be obtained with just the paraboloid. The circle of intersection of the two surfaces is 3.500 inches in diameter, and the projected area of the paraboloid on a plane perpendicular to the axis, the aperture of the system, is 2.14 cm^2. The focal point where light incident parallel to the axis actually converges is 25.027 inches from the center of the circle of intersection.

Figure 23 is a photograph of the disassembled components used with the telescope; they are, from left to right: stop, telescope, mounting, sliding tube for focusing with G-M counter on top, and G-M counter in its holder. These essential optical elements of the telescope assembly are similar in size and structure and serve the same purpose as the ones described under collimators. The alignment of the apparatus is obtained in an identical manner.

4.6.4 Pinhole Camera. Figure 24 is a photograph of the pinhole camera. The pinhole camera is a form of geometrical collimator that permits the resolution of detail within the field of view. In order to achieve an angular resolution of one minute of arc, a pinhole with a diameter of 0.0079 ± 0.0002 inch was drilled in a 0.005 inch thick brass sheet. The brass sheet with the pinhole at the center was cut to a size of 2 inches by 2 inches and was attached to a stop with a central opening of 0.5 inch diameter. This stop was placed in front of the optical apparatus described previously. The X-ray film in its cassette was attached to the focusing tube, replacing the diaphragm. The distance between the film and the pinhole was approximately 27 inches.

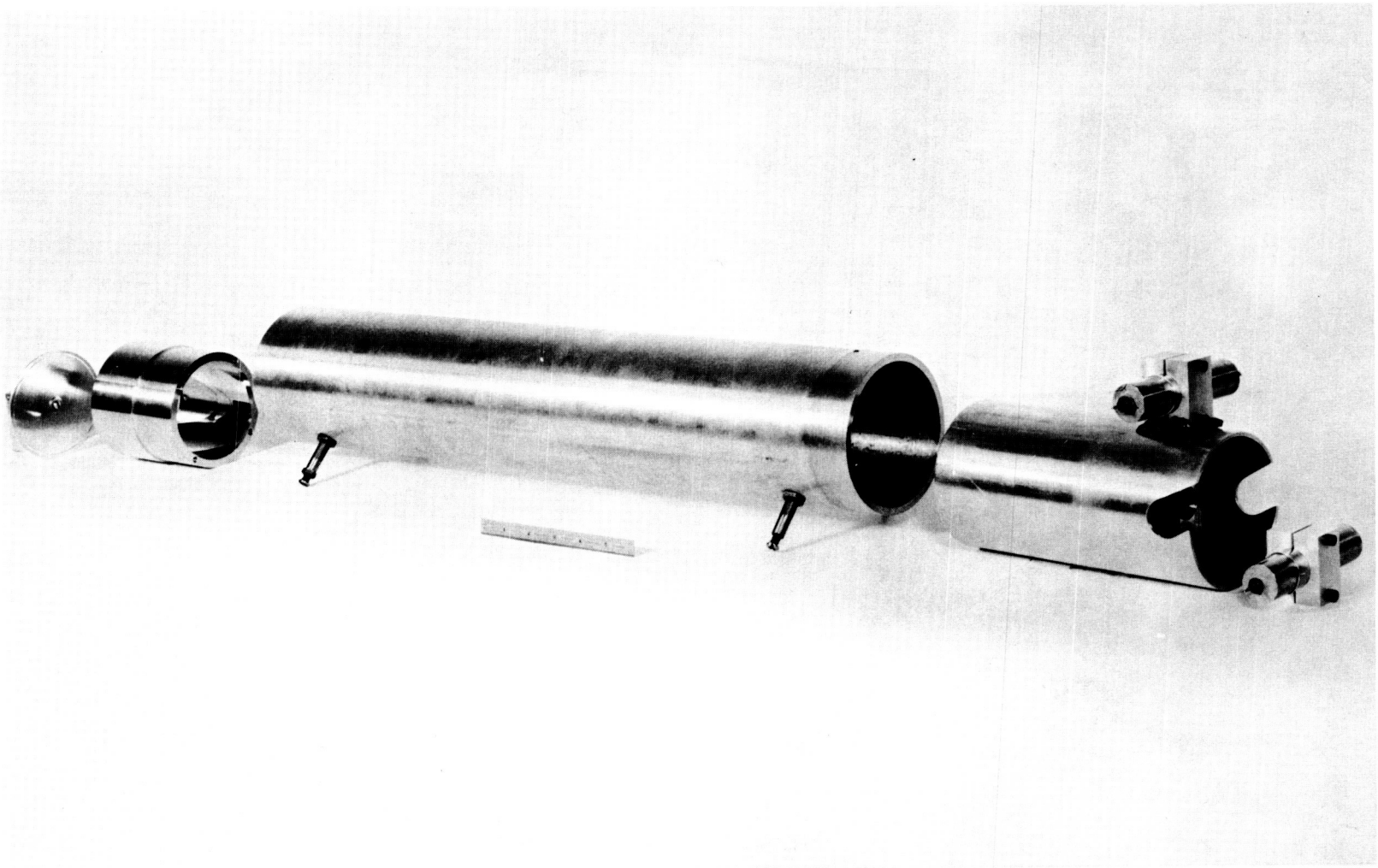

Figure 23 Exploded View of Telescope Assembly

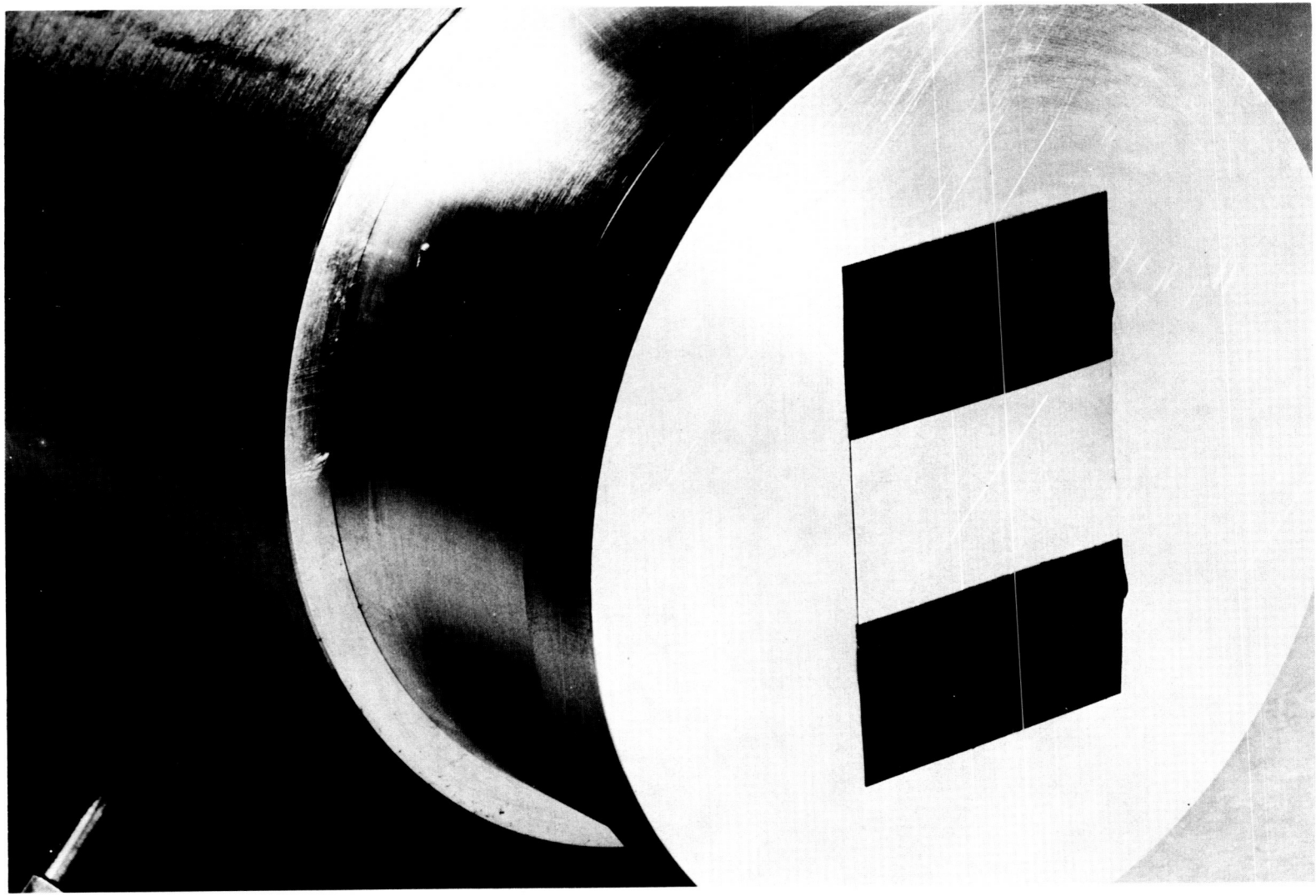

Figure 24 Pinhole Camera

5.0 EXPERIMENTAL WORK

The scope of the experimental work described in this report encompasses the construction and testing of a collimator and a telescope for soft X-rays for astronomical use, and the determination of the X-ray reflectivity of various practical surfaces used with these devices. To these ends, the angular resolutions of the glass and steel cone collimators and machined aluminum telescope and the efficiency of these devices at two wavelength ranges and a variety of conditions of the reflecting surfaces were measured.

5.1 Angular Resolution Measurements

The measurement of the angular resolution of the glass cone collimator was done in the following way. The collimator, at the end of the long pipe, was aligned with the aid of a concentrated arc lamp at the position of the X-ray source in the large vacuum chamber so that the light reflected from the conical surface passed through a one millimeter hole in a diaphragm about 10 inches behind the cone where the light concentrated to the smallest spot. An annular slit in front of the collimator allowed radiation to reach the conical surface, but stopped direct radiation from passing through the aperture from the source. A Geiger counter with a .00025 inch thick mylar window was placed behind the aperture to detect X-radiation passing through. Figure 21 illustrates this arrangement.

Another Geiger counter with an extra layer of .00025 inch mylar over its window for attenuation was placed in the large vacuum chamber about one meter from the X-ray source to monitor the X-ray flux for purposes of normalization. When the X-ray source is moved by means of the screw mechanism, the collimated spot deforms into a circle, less and less of which overlaps the aperture the further the source is moved. A plot of the normalized counting rate, corrected for background, is given in Figure 25. The shape of the distribution closely follows the curve that can be calculated from geometrical optics considerations alone by taking into account the

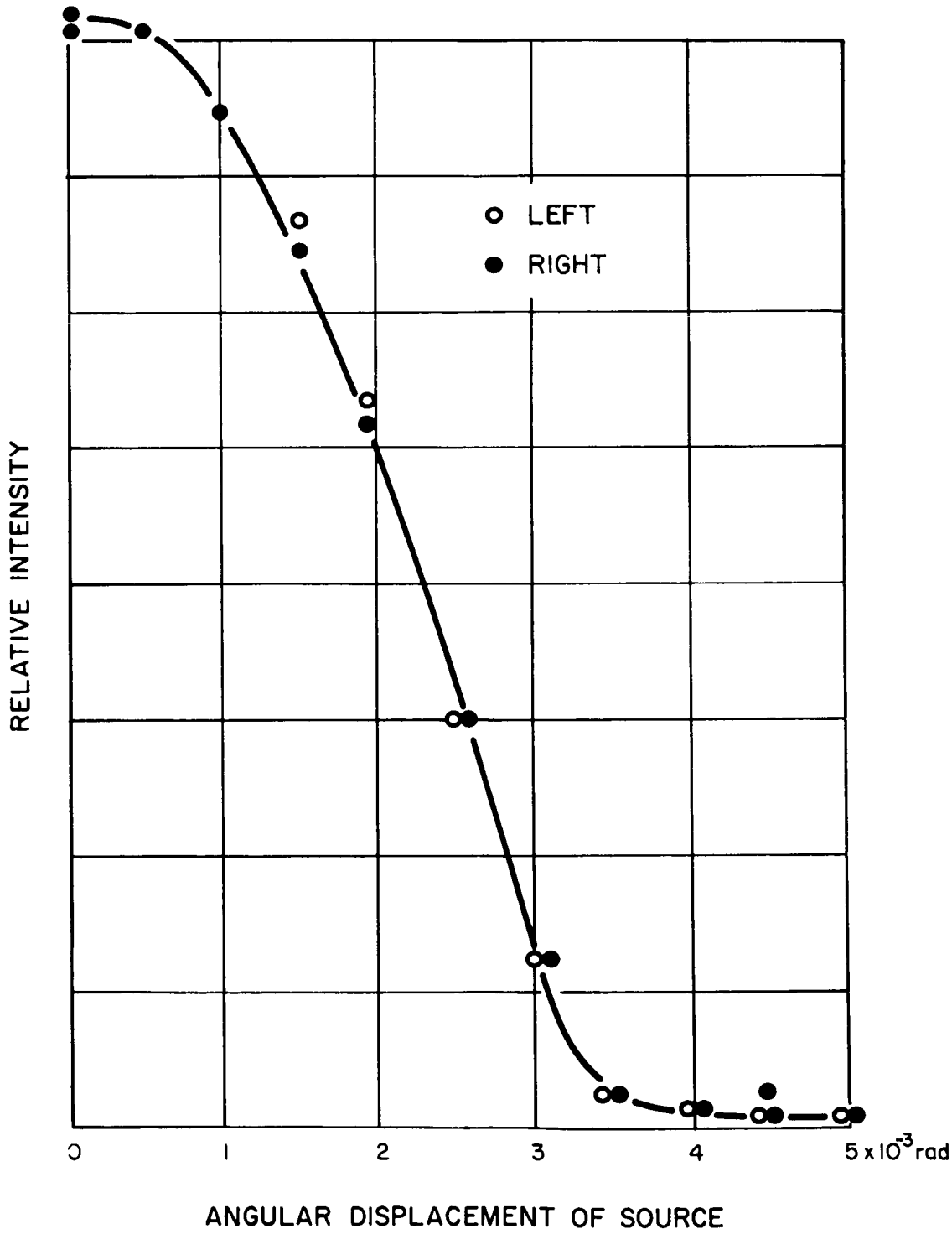

Figure 25 Angular Resolution of Glass Cone Collimator

finite width of the aperture. There is evidence for a small amount of diffuse scattering. Figure 26 shows the results of the same experiment done with the steel cone collimator. The amount of radiation diffusely scattered is much greater due presumably to the much rougher surface of the steel. The half-width of both curves is about 4 milliradians, as predicted by considering the finite size of the smallest spot which can be obtained from these devices (1 mm) and their focal length (250 mm).

The same experiment was performed with the image-forming telescopes. The resolution curve shown in Figure 27 is in agreement with the expected distribution computed on the basis of geometrical optics, taking into account the 1 mm aperture width in front of the Geiger counter and the focal length of about 650 mm. A more precise determination of resolution with this device is obtained by means of the X-ray photograph described below which shows a resolution of the order of 1 minute of arc. The reason why Geiger counters with small apertures were not used is that the problem of alignment became increasingly difficult with smaller and smaller apertures, and it was therefore more convenient to rely on the measurement obtained by the photographic technique which did not necessitate such alignment. The tails of the distributions observed are quite noticeable, both for the cones and for the telescope. The diffused halo which appears in the photograph around the image of each spot is a direct representation of this fact. This diffused halo is believed to be due to imperfections in the polishing of the telescope. This instrumental effect can be reduced perhaps to the theoretical limits by use of more accurate fabrication techniques such as employed in the construction of optical instruments.

5.2 Measurements of Efficiency

We define the efficiency of a collimator, or telescope, as the ratio of the flux focused by the device into the focal point to the flux entering the aperture of the device. The efficiency of the devices for soft X-rays was measured under various conditions with the apparatus arranged as shown in Figures 7, 20, and 23. One Geiger counter was positioned above the telescope or collimator assembly to measure the flux incident on the device being tested, and another placed at its focus, where X-rays from the source are concentrated. From the counting rates of the two counters, and the

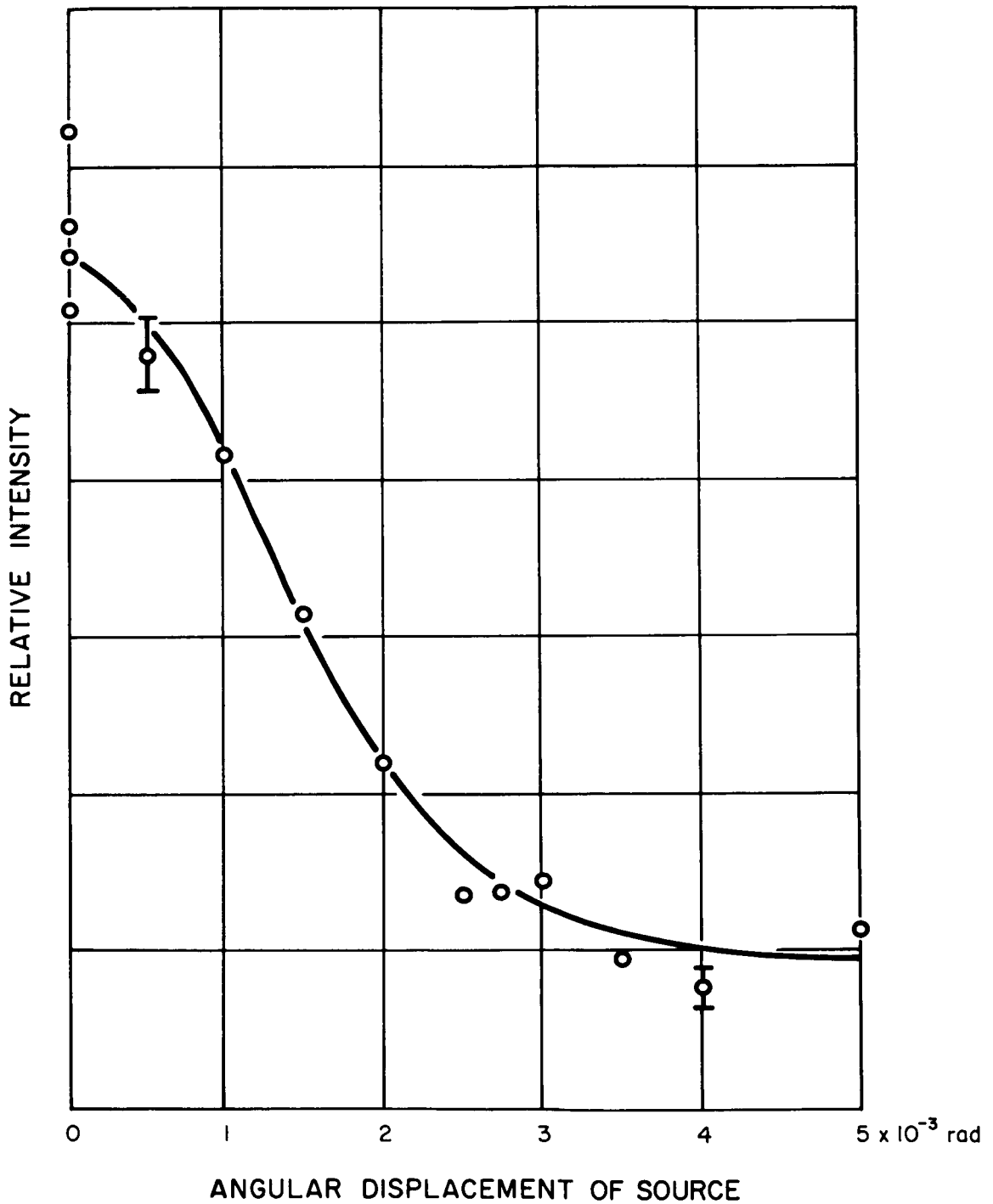

Figure 26 Angular Resolution of Steel Cone Collimator

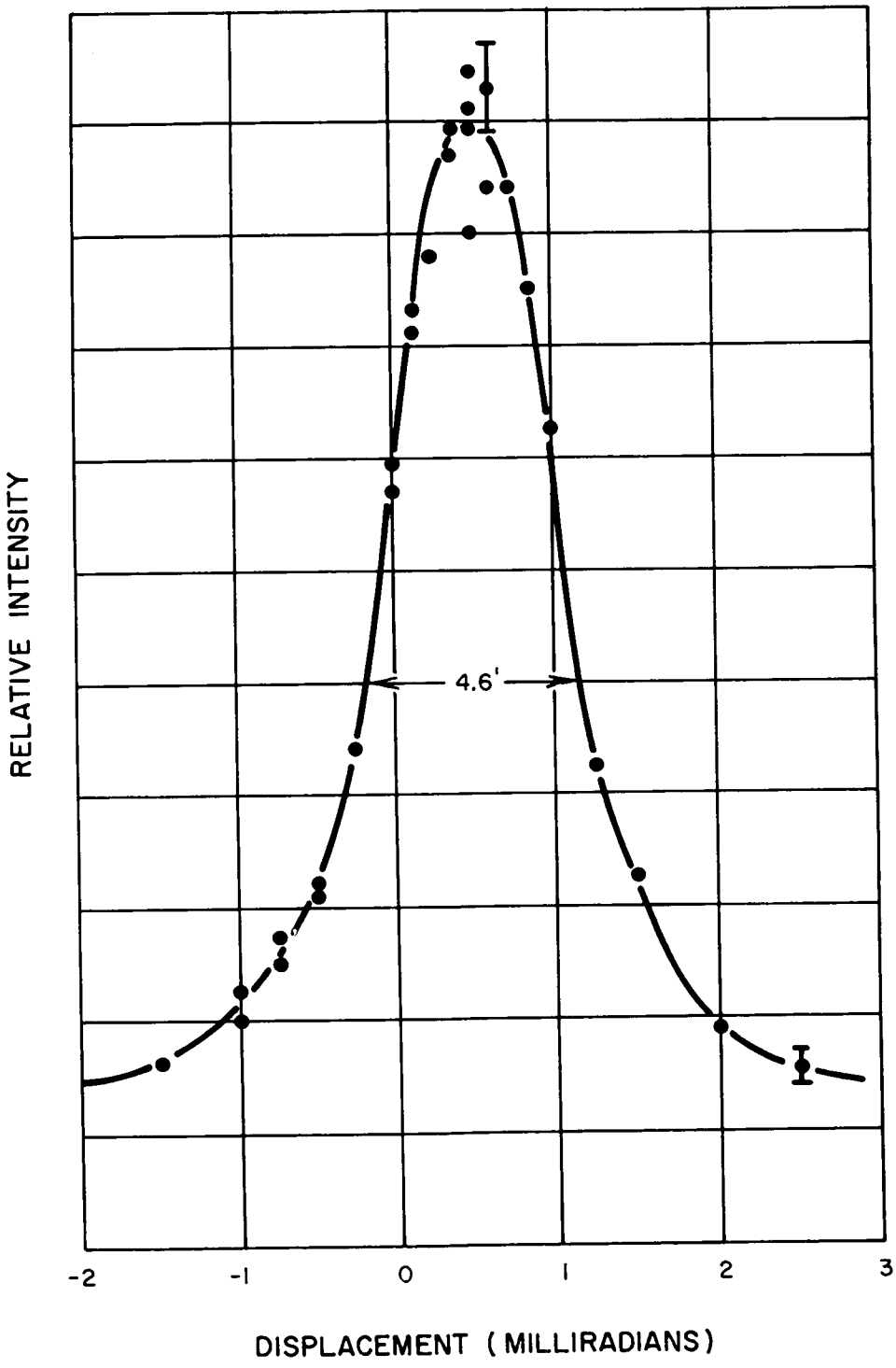

Figure 27 Resolution of Aluminum Telescope

apertures of the telescope or collimator and the area of the window of the auxiliary counter (that of the counter on top), the efficiency E may readily be computed (for monochromatic incident radiation)

$$E = \frac{N_{Tel} \quad A_{GT}}{N_{GT} \quad A_{Tel}}$$

where E is the efficiency, A_{GT} and A_{Tel} are the apertures of the auxiliary Geiger counter and the telescope, respectively, and N_{Tel} and N_{GT} are the number of counts registered in a given time interval by the counter at the focal point of the telescope and by the auxiliary counter, respectively. In practice, the two counters were interchanged several times so that possible differences in sensitivity could be corrected for, and the reproducibility of the measurements shown. Measurements were made utilizing the X-ray source shown in Figure 13. This source is, of course, not monochromatic. Results for such measurements under various conditions are shown in Table 1. These values should be interpreted as giving a qualitative appraisal of the performance of the instrument. No statistical errors are shown because the statistical errors of each measurement were much smaller than the variation between repeated measurements. This effect could be due to a variety of causes: for instance, changes in the emission characteristics of the X-ray source and to degradation of the polished surfaces due to repeated exposure to air. Additional causes of error are occasional misalignments or degradation of the detectors during a particular run.

Two points must be borne in mind with respect to the results for the image-forming telescope. First, X-rays undergo two reflections, so that reflection losses are necessarily greater than for a simple paraboloidal or conical collimator, other things being equal. In fact, the efficiency of a two-reflection device is to first approximation given by the product of the efficiency for each reflection. Second, the source of the X-rays was at 400 inches, from the telescope rather than at infinity. Consequently, X-rays were incident on the reflecting surface at an angle of about 4 milliradians from the axis. As can be seen from Figure 5. the efficiency with which a plane aluminum surface reflects 8.32 A radiation decreases markedly if the angle of incidence is increased by 4 milliradians from the 17.5 milliradians (one degree) for which the telescope was designed.

Table I

DEVICE	SURFACE	EFFICIENCY (%)	
		8 to 12 A	~44 A
A. Telescope	1) #1 Nickel Plated		1.5
	2) #1 Chromium Plated		7.0
	3) #2 Plished Aluminum		17.0
	4) #2 Evaporated Gold	0.5	2.4
	5) #2 Repolished Aluminum	.25	3.0
	6) #3 Polished Aluminum	.20	5.0
	7) Cast Epoxy		4.5
	8) Cast Epoxy with Evaporated Aluminum		2.0
B. Collimator	Glass		46.0
	Steel		2.0

Taking the double reflection into account, this effect alone would reduce the efficiency of an ideal instrument from 36% to 4%, for 8.32 A radiation.

5.3 Surface Preparation

Several telescopes of the same geometry were made and tested, including three machined from aluminum and one cast from aluminum-filled epoxy. Since the efficiencies were somewhat less than would be expected for ideal surfaces at each wavelength, attempts were made to improve the surfaces by polishing and coating with materials of higher atomic number. As listed in Table I, the first aluminum telescope was nickel plated, and the nickel plating buffed. Then a thin plating of chromium was applied. The second aluminum telescope seemed to have a good smooth surface, and we tried to improve its efficiency by evaporating a layer of gold onto it. This was done with conventional vacuum evaporation apparatus set up so that the gold was evaporated from a point in the middle of the telescope. When the gold was removed, the aluminum underneath was found to be tarnished in places. When it was repolished, the efficiency fell sharply from what it was before gold was evaporated on it. The third aluminum telescope had a rather dull surface originally because it had been polished with a coarse compound to remove two deep scratches put into the surface when it was machined. Much additional polishing was needed to make the surface shiny. The epoxy telescope is discussed in more detail below. The aluminum was evaporated on it in the same manner that gold was evaporated onto the aluminum telescope.

5.4 Wavelength of Incident Radiation

The measurements identified as 8 to 12 A were made using an aluminum anode in the X-ray source, which was operated at 3000 volts, and .00025 inch aluminum filters in front of the counters. Figure 28 shows the decrease of intensity when additional thicknesses are added. From this data and the known thickness of the Al filter, an absorption coefficient can be calculated. Taking into account the short wavelength cut-off, it can be shown that the transmitted radiation falls in the 8 to 12 A range (see Figure 29).

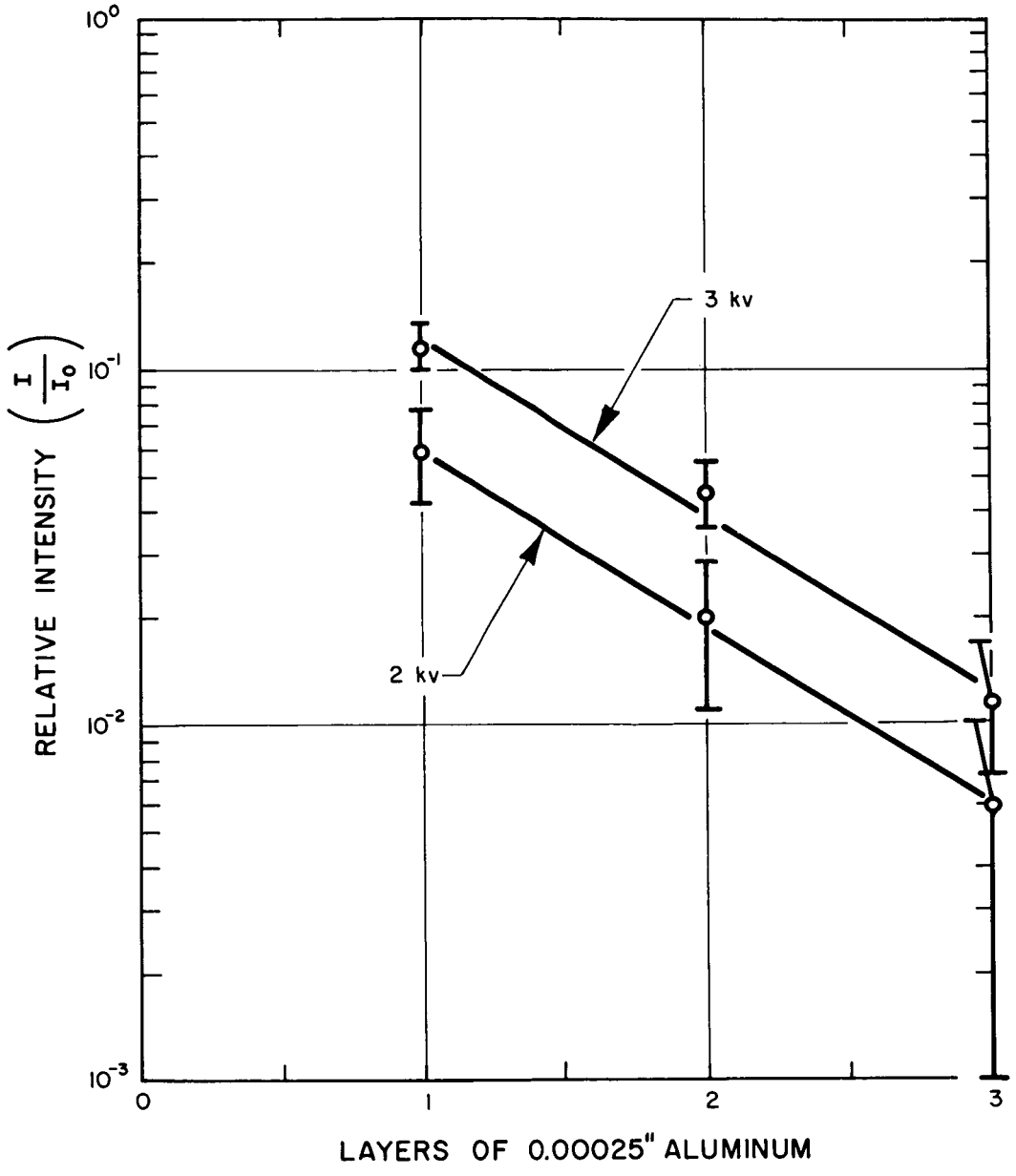

Figure 28 Attenuation Curve

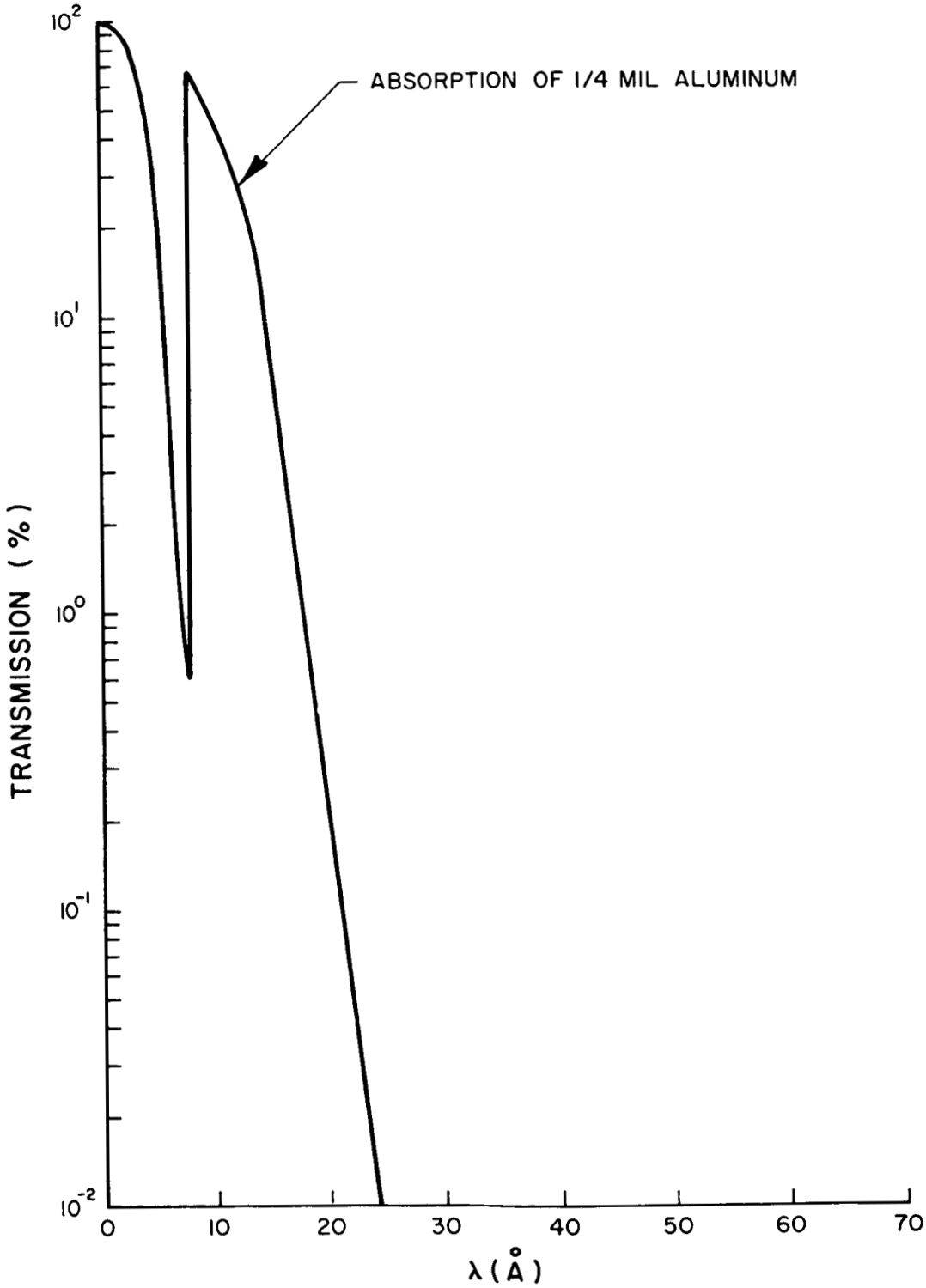

Figure 29 Transmission of Aluminum Filter vs Wavelength

The measurements at 44 A were made with a carbon anode operated at 1500 volts. Some of the hard component of the continum would be detected by our Geiger counters. Its effect would be to make the efficiencies we measured lower than they actually are for the CK_α line. The hard component could not be eliminated without reducing intensities below a practical level. The measurement of efficiency for the CK_α radiation represents therefore a lower bound. These two wavelength intervals were chosen, apart from experimental convenience, because the shorter one represents the minimum wavelength at which these telescopes were designed to operate, and the longer wavelength represents a value for which the telescopes should already have reached their maximum efficiency.

5.5 Optical Characteristics

Using the image-forming telescope, photographs were taken with X-rays in the region about 8 to 12 Å from our large area source and our point source, shown in Figure 30 a, b and c. These photographs show the image-forming properties of the device, its resolution, and its field of view. The first two were obtained with Kodak ultra-speed dental X-ray film, the third with DuPont 508 medical X-ray film, and Figure 30 d and other photographs were taken with Ilford G industrial X-ray film. The cassette window was .00025 inch aluminum to keep out visible light and to provide filtration so that only radiation in the 8 to 10 Å range will be registered. The large area source was operated at 2500 volts and 10 milliamperes with an exposure of an hour. The point source was operated at 3000 volts, and the exposure was monitored by a Geiger counter with an .00025 inch aluminum filter at the same distance as the telescope. Experience showed that when this counter had registered 100,000 counts, a usefully dark spot would be formed on the developed film.

Figure 30 a and b were taken with the large area source. In Figure 30 b, strips of brass 1/16", 1/8" and 1/4" wide, subtending angles at the telescope of about 1/2, 1 and 2 minutes of arc, were placed in front of the source to show its resolution. The lack of contrast in this photograph is presumably due to scattering of X-radiation from the extended source against the walls of the vacuum pipe in which the telescope is placed as well as under-exposure.

A. X-Ray Image of an Extended Source Formed by the Telescope

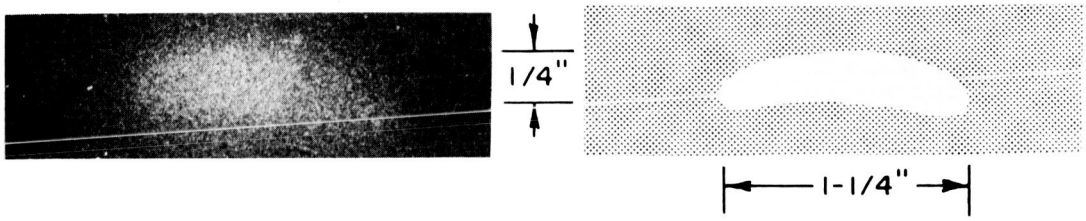

X-ray photograph of extended source 1-1/4" x 1/4" at a distance of 400" from the telescope using aluminum filters.

B. X-Ray Images of Several Extended Sources Formed by the Telescope

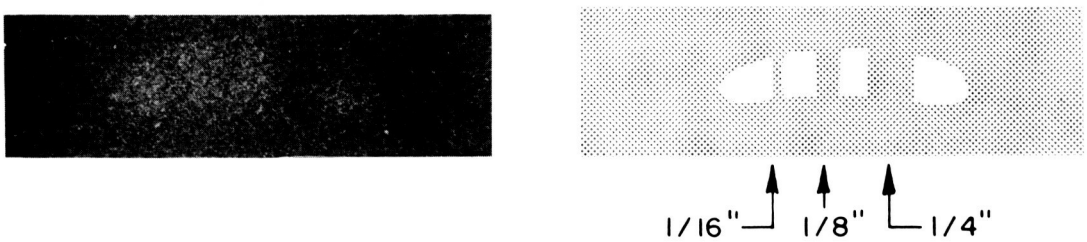

The same source at the same distance as in Figure A. Opaque bars 1/16", 1/8" and 1/4" in front of it. Aluminum filters were used.

Figure 30-A, B Experimental Photographs

C. X-Ray Images of Several Extended Sources Formed by the Telescope

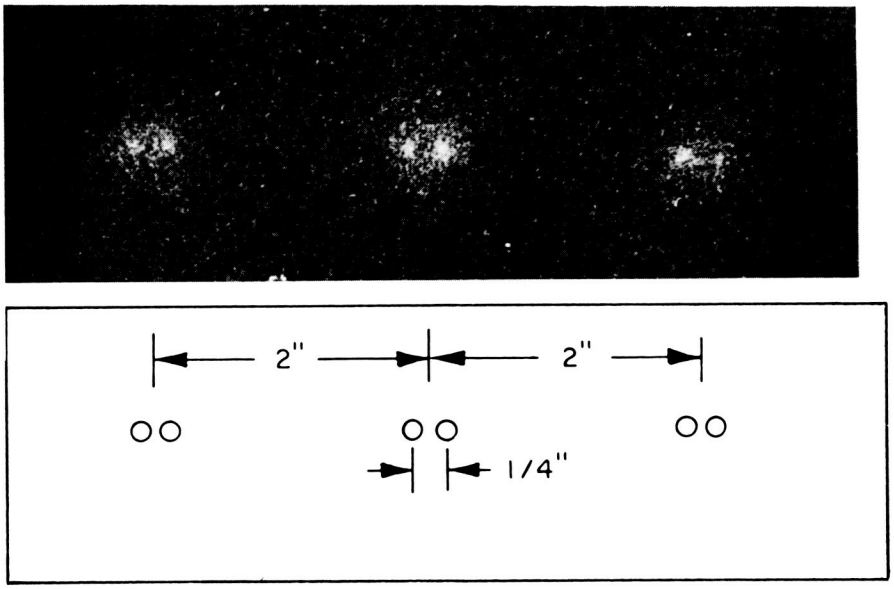

Images of a point X-ray source (diameter approximately 0.01"). The source was moved 1/4" between exposures of adjacent dots, and 2" between outer and central pairs. The source was at a distance of 400" from the telescope. During exposure the following number of photons were monitored by a G-M counter at 400" from the source: from left to right 80,000, 90,000, 104,000, 140,000, 96,000, and 70,000 photon counts. The wavelength of the radiation was about 8 to 20 A.

D. Pinhole Camera Picture of Point Sources

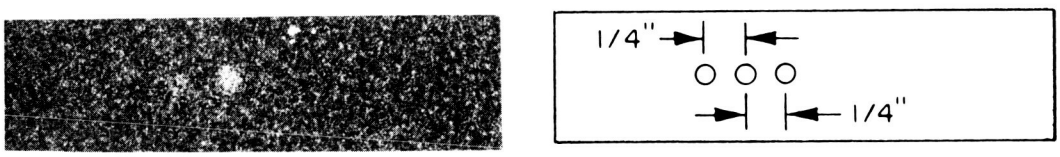

Same source and separation between dots with pinhole camera of identical resolution for 100,000, 300,000 and 900,000 monitored photon counts.

Figure 30-C, D Experimental Photographs

Figure 30 c was made with the point source by moving it successively across, producing good surfaces for normal reflection of visible light. We have attempted to adapt this technique to our grazing incidence mirrors. Preliminary results indicate that the method shows great promise. This technique, if perfected, would, of course, have great practical advantages.

Epoxy resins adhere tenaciously to most surfaces, and the first problem is to find a mold release so that the finished casting may be separated from the mold. In casting replica mirrors, the mold release was an evaporated coating of silver which would strip from the pyrex mold when the casting was pulled away. The silver adhering to the epoxy could be removed with nitric acid, leaving a surface substantially as smooth as that of the original from which it was molded. However, the difficulty of evenly covering a mold of cylindrical form with evaporated silver, and the difficulty of pulling it away from the casting at an angle parallel to the adhering surfaces prompted us to try another sort of mold release. This was a silicone varnish - Dow Corning R-671. It has a low viscosity so that when it is applied to the mold, which is machined from aluminum to the desired shape and polish, it flows evenly over the surface. Its surface tension causes the surface of the varnish to be smoother than the surface of the mold. The varnish is cured by heating the coated mold to 340° for 16 hours, and it forms a tough adherent coating to which epoxy will not bond.

The inner mold was, as we have said, machined from aluminum to the negative shape of the inside surfaces of the aluminum telescope. The outer mold was made flexible to avoid straining the casting. It was itself cast, using an aluminum telescope as a mold, from Eccosil 4712 epoxy-silicone rubber using catalyst 27, both products of Emerson & Cuming, Inc., and cured for two hours at 250°F. This material is a flexible potting compound, and was chosen because it retains its flexibility after prolonged exposure to elevated temperatures. The inside of this flexible mold is coated with an ordinary teflon mold release.

The telescope is cast from Emerson & Cuming, Inc., Eccobild 421 MM epoxy casting compound. This epoxy resin is filled with aluminum powder, and is a dimensionally stable type designed especially for casting. The epoxy and its catalyst, catalyst 211, were warmed and then outgassed by being placed in a vacuum. The mixture was then poured into the assembled mold, and put into an

oven for curing at 170° F for 16 hours. The cured epoxy has a coefficient of thermal expansion greater than aluminum, so that at the end of cure the assembly is heated above the curing temperature, removed from the oven, and the inner mold driven out. Figure 31 shows the finished telescope (extreme right) and the mold with which it was made.

The method has several difficulties to be overcome. First, the mold release deteriorates with use. It tends to get scratched in freeing the telescope, and after it has been heated several times, it darkens and its surface loses its smoothness. Unfortunately, it is impossible to remove the varnish except with abrasives. A similar product, not yet evaluated, exists, which can be removed with solvents. Second, because of the differences in thermal coefficients of expansion, strains develop which may lead to cracking when the inner mold is removed. This problem can be avoided by careful technique during mold removal. Third, the reflecting surfaces are marred by the effects of very small bubbles, dust, and a few varnish drips that did not run off or smooth themselves out. These problems too can be overcome by careful technique in applying the varnish, avoiding dust, and pouring the epoxy resin into the mold. Finally, there is the problem of coating the epoxy surface with an evaporated coating of aluminum or gold, for instance, to form a surface of a material with a higher atomic number for better reflection at larger grazing angles or shorter wavelengths. While in our experience, although the evaporated coating appears shiny, it is significantly rougher than the surface to which it applied; this is not so generally with evaporated coatings, and there seems to be no reason why we cannot apply a coating about as smooth as the substrate, even though the source of metal is rather closer to the surface onto which it is deposited than is usual for metallic evaporation.

For the epoxy replicas, we note, the efficiency is as good or better than that which we obtained with our machined telescope, in spite of the preliminary state of development, and in spite of the low atomic number of the elements composing the epoxy-hydrogen, carbon and oxygen.

Successful manufacture of the cast telescopes, would be extremely useful. They have the advantage of light weight and low unit cost if several are manufactured. From one mold any number of identical units could be made. They are dimensionally stable, and suitable for use in high vacuum equipment or space.

Figure 31 Telescope Mold and Product

6.0 DISCUSSION OF RESULTS

6.1 Angular Resolution

The angular resolution for the collimators and the telescopes was finer than could be measured utilizing a small aperture Geiger counter. However, evidence of diffuse scattering of the radiation from imperfections in the reflecting surface was found. This effect was smallest in the case of the glass cone whose surface had been prepared by standard optical glass polishing techniques. It is therefore apparent that this diffuse scattering can be diminished by proper preparation of the reflecting surfaces which in the present case were simply machined and polished with standard metal polishing techniques.

The measured angular resolution of the telescope as determined by the photographic technique is about 1 minute of arc, which is finer or comparable to the accuracy of the existing pointing controls of satellites and rockets.

As discussed in Section 2.4, the ultimate resolution of a telescope of this particular design is a few seconds of arc. Since the resolution of the present instrument, even though roughly constructed, is sufficient to be useful, we feel that further improvement may be possible, allowing us to indeed reach resolutions close to the theoretical limit.

6.2 Efficiency

The measured efficiencies as shown in Table I are in most cases considerably smaller than the predicted theoretical limit. It is worth noting that measurements performed with the glass cone collimator yielded results in rough agreement with the theoretical expectation. The efficiency of the steel cone collimator on the other

hand was found to be considerably smaller than expected. We believe that the integrated number of photons, including those reflected diffusely about the focal spot, is about the same in both cases. In the case of the steel cone collimator, however, most of the reflected intensity falls out of the aperture in the focal plane.

We believe also that diffuse scattering is responsible for the difference between the measured efficiencies of the telescopes and the expected values. This diffuse scattering could be due either to gross imperfections in the shape of the surface or to its roughness. The electroplating of metal coatings on these surfaces as well as the evaporation of metals on them seemed to worsen rather than improve the situation. This could be due to increased departure of the figure from the desired shape or from added roughness and discontinuities in the surface introduced by the processes themselves. One of the problems is that one cannot depend upon improving any of these surfaces with polishing. As a result of this conclusion, it was felt that some new approach had to be tried.

Due to the difficulty of obtaining the desired telescope fabricated out of glass, and the relative ease in building a negative of the desired surface by optical glass techniques, we decided to experiment with casting. The success of the early measurements performed with cast surfaces seems to indicate that such a method can give reflecting elements which are as perfect as the original. An optically correct glass negative will therefore allow us to construct reproducible telescopes much improved over the ones which have been used in the present research program.

6.3 Spectral Response

The response of these devices with wavelength was not in contradiction with the predicted behavior. The cut-off at shorter wavelength seems to be somewhat more drastic than expected, resulting in extremely low efficiencies toward the design limits of the instrument, 8 Å. It should be noted that the spectral range of operation depends entirely on the chosen design parameters — in particular the angle of incidence. Total reflection has been shown to occur with efficiencies close to the theoretically predicted efficiencies down to 1.34 Å (ref. 9).

We hope that with improved techniques of fabrication to be able to extend the range of usefulness of this type of X-ray optics down to a few Angstroms.

6.4 Optical Characteristics

The optical properties of these instruments and in particular the field of view, were shown to be satisfactory for solar astronomy. No appreciable distortions were noted within the field of view. In particular, the field of view of the instruments can be made large enough to include a substantial portion of the solar corona as well as the solar disc.

7.0 CONCLUSIONS AND RECOMMENDATIONS

In the course of this research program the feasibility of constructing total reflection optics suitable for X-ray astronomy has been demonstrated. In the course of the experiment the first successful photograph in the 8 to 12 Å range, to be taken with such fine angular resolution, high speed, and a large field of view was obtained.

Our experiments have shown that the glass cone collimator and the image-forming telescopes are useful instruments in detecting soft X-rays with a high degree of resolution while still retaining the advantage of a much larger aperture than a pinhole camera affords. For example, the efficiency of 0.5% in the 8 to 10 Å range for the gold covered aluminum telescope, given its 2.14 cm^2 aperture, means that a camera using that telescope would be about thirty times faster than a pinhole camera with the same 1 minute of arc resolution. 5% efficiency typical of the 40 to 60 Å region would mean a camera 300 times faster than the corresponding pinhole camera. As the technique improves, one can hope to reach the theoretical gains which are of the order of thousands, even for the small telescopes studied during this program.

In applications where the instrument is to be scanned mechanically across the field of view, the collimator is ideally suited. With but a single reflection involved, the efficiency is inherently greater than it can be for the double reflecting image-forming device.

The resolution of the telescope, as determined directly from X-ray photographs taken in the 8 to 12 Å region, is about 1 minute of arc, or 1/30 the angular diameter of the Sun. The significance of this is that the device is a practical instrument for solar X-ray astronomy in its present state of development, with marked advantages over the pinhole camera or the Fresnal zone plate for studying the structure of the soft X-ray emitting regions on the solar surface.

We believe that feasibility of the total reflection techniques has been sufficiently demonstrated, and the performance of the device proven, to justify the design and construction of flight hardware for astronomical observations. It is our hope that experiments will be performed utilizing the results of this development work and that scientists of American Science and Engineering, Inc., will be permitted to collaborate in such programs.

December, 1964
American Science and Engineering, Inc.
11 Carleton Street
Cambridge 42, Massachusetts

REFERENCES

(1) R. Giacconi and B. Rossi, J. Geophys. Res. 65, 773 (1960).

(2) T. R. Burnight, Phys. Rev. 76, 165 (1949).

(3) H. Friedman, Reports on Progress in Physics 25, 163 (1962).

(4) P. Kirkpatrick and A. V. Baez, J. Opt. Soc. Am. 39, 746 (1949).

(5) P. Kirkpatrick and H. H. Pattee, Jr., in S. Flugge, Handbook der Physik, Vol. 30, Springer-Verlag, Berlin (1957) p. 324.

(6) H. Wolter, Ann. der Physik 10, 94 (1952).

(7) R. W. Hendrick, J. Opt. Soc. Am. 47, 165 (1957).

(8) L. G. Parratt, Phys. Rev. 95, 359 (1954).

(9) R. C. Duncan and L. G. Parratt, AFOSR TN-58-680, ASTIA AD 162 212 (1958).

(10) B. L. Henke in A. Engstrom et al., X-Ray Microscopy and Microanalysis, Elsevier, Amsterdam (1960) p. 10.

(11) R. F. Wuerker, Third International Symposium on X-Ray Optics and X-Ray Microanalysis, Stanford (1962) (Unpublished).

(12) B. L. Henke, in W. M. Mueller, Advances in X-Ray Analysis, Vol. 4, Plenum Press, New York (1961) p. 244.